as acute-phase kinetics that responds to a combination of injury and the presence of microorganisms, exhibits striking similarities to the vertebrate acute-phase response [12,23]. The later response, however, appears to respond to increasing bacterial load. *L. monocytogenes* was found to grow exponentially in infected flies, increasing approximately 10-fold in *Canton-S* and 150-fold in *white* just 1 day after infection (data not shown). The later response appears to respond to growing *L. monocytogenes* that escaped early responses of host innate immunity. Considering activation levels of immunity are equal between wild-type lines by the later response, our results provide the first experimental evidence that variation in immune activity during early responses could regulate variation in susceptibility of wild-type *Drosophila* (Fig. 4).

## Acknowledgments

## Appendix A. Supplementary data

Supplementary data associated with this article can be found, in the online version, at doi:10.1016/j.bbrc.2008.11.097.

## References

[1] G.S. Cooke, A.V. Hill, Genetics of susceptibility to human infectious disease, Nat. Rev. Genet. 2 (2001) 967–977.
[2] M.J. Williams, Regulation of antibacterial and antifungal innate immunity in fruitflies and humans, Adv. Immunol. 79 (2001) 225–259.
[3] J.A. Hoffmann, J.-M. Reichhart, *Drosophila* innate immunity: an evolutionary perspective, Nat. Immunol. 3 (2002) 121–126.
[4] B.P. Lazzaro, B.K. Sceurman, A.G. Clark, Genetic basis of natural variation in *D. melanogaster* antibacterial immunity, Science 303 (2004) 1873–1876.
[5] J.A. Hoffmann, The immune response of *Drosophila*, Nature 426 (2003) 33–38.
[6] B.E. Mansfield, M.S. Dionne, D.S. Schneider, N.E. Freitag, Exploration of host-pathogen interactions using *Listeria monocytogenes* and *Drosophila melanogaster*, Cell. Microbiol. 5 (2003) 901–911.
[7] A. Takehana, T. Katsuyama, T. Yano, Y. Oshima, H. Takada, T. Aigaki, S. Kurata, Overexpression of a pattern-recognition receptor, peptidoglycan-recognition protein-LE, activates imd/relish-mediated antibacterial defense and the prophenoloxidase cascade in *Drosophila* larvae, Proc. Natl. Acad. Sci. USA 99 (2002) 13705–13710.
[8] N.E. Freitag, L. Rong, D.A. Portnoy, Regulation of the prfA transcriptional activator of *Listeria monocytogenes*: multiple promoter elements contribute to intracellular growth and cell-to-cell spread, Infect. Immun. 61 (1993) 2537–2544.
[9] S.M. Brandt, M.S. Dionne, R.S. Khush, L.N. Pham, T.J. Vigdal, D.S. Schneider, Secreted bacterial effectors and host-produced Eiger/TNF drive death in a *Salmonella*-infected fruit fly, PloS Biol. 2 (2004) e418.
[10] H. Hamamoto, K. Kurokawa, C. Kaito, K. Kamura, I.M. Razanajatovo, H. Kusuhara, T. Santa, K. Sekimizu, Quantitative evaluation of the therapeutic effects of antibiotics using silkworms infected with human pathogenic microorganisms, Antimicrob. Agents Chemother. 48 (2004) 774–779.
[11] M.S. Dionne, N. Ghori, D.S. Schneider, *Drosophila melanogaster* is a genetically tractable model host for *Mycobacterium marinum*, Infect. Immun. 71 (2003) 3540–3550.
[12] B. Lemaitre, J.M. Reichhart, J.A. Hoffmann, *Drosophila* host defense: differential induction of antimicrobial peptide genes after infection by various classes of microorganisms, Proc. Natl. Acad. Sci. USA 94 (1997) 14614–14619.
[13] P.A. Campbell, B.P. Canono, D.A. Drevets, Measurement of bacterial ingestion and killing by macrophages, in: J.E. Coligan et al. (Eds.), Current Protocols in Immunology, John Wiley and Sons Inc., New Jersey, 1994. UNIT 14.6.
[14] E.D. Gregorio, S.J. Han, W.J. Lee, M.J. Baek, T. Osaki, S. Kawabata, B.L. Lee, S. Iwanaga, B. Lemaitre, P.T. Brey, An immune-responsive Serpin regulates the melanization cascade in *Drosophila*, Dev. Cell 3 (2002) 581–592.
[15] S.E. McGuire, P.T. Le, A.J. Osborn, K. Matsumoto, R.L. Davis, Spatiotemporal rescue of memory dysfunction in *Drosophila*, Science 302 (2003) 1765–1768.
[16] A.J. Needham, M. Kibart, H. Crossley, P.W. Ingham, S.J. Foster, *Drosophila melanogaster* as a model host for *Staphylococcus aureus* infection, Microbiology 150 (2004) 2347–2355.
[17] V.C. Harris, K.E. Habel, F.G. Ali, D.E.L. Promislow, Alternative measures of response to *Pseudomonas aeruginosa* infection in *Drosophila melanogaster*, J. Evol. Biol. 20 (2007) 526–533.
[18] B. Lemaitre, J. Hoffmann, The host defense of *Drosophila melanogaster*, Annu. Rev. Immunol. 25 (2007) 697–743.
[19] K. Soderhall, L. Cerenius, Role of the prophenoloxidase-activating system in invertebrate immunity, Curr. Opin. Immunol. 10 (1998) 23–28.
[20] M. Meister, M. Lagueux, *Drosophila* blood cells, Cell. Microbiol. 5 (2003) 573–580.
[21] T. Yano, S. Mita, H. Ohmori, Y. Oshima, . Fujimoto, R. Ueda, H. Takada, W.E. Goldman, K. Fukase, N. Silverman, T. Yoshimori, S. Kurata, Autophagic control of Listeria through intracellular innate immune recognition in *Drosophila*, Nat. Immunol. 9 (2008) 908–916.
[22] S. Kurata, Recognition of infectious non-self and activation of immune responses by peptidoglycan recognition protein (PGRP)-family members in *Drosophila*, Dev. Comp. Immunol. 28 (2004) 89–95.
[23] A.H. Jules, Innate immunity of insects, Curr. Opin. Immunol. 7 (1995) 4–10.

ELSEVIER

# Rapid identification of virus-carrying mosquitoes using reverse transcription-loop-mediated isothermal amplification

Namal Perera [a,b], Hiroka Aonuma [a,c], Aya Yoshimura [a], Tokiyasu Teramoto [a], Hiroshi Iseki [a], Bryce Nelson [a], Ikuo Igarashi [a], Takeshi Yagi [c], Shinya Fukumoto [a,*], Hirotaka Kanuka [a,*]

[a] National Research Center for Protozoan Diseases, Obihiro University of Agriculture and Veterinary Medicine, Inada-cho, Obihiro, Hokkaido 080-8555, Japan
[b] Medical Research Institute, Colombo-08, Sri Lanka
[c] KOKORO Biology Group, Laboratories for Integrated Biology, Graduate School of Frontier Biosciences, Osaka University, Suita, Osaka 565-0871, Japan

## ABSTRACT

Mosquitoes are critical vectors in many arboviral transmission cycles. Considering the increasing incidence of arboviral infections throughout the world, monitoring of vector populations for the presence of an arbovirus could be considered an important initial step of risk assessment to humans and animals. In response to this need, increased efforts to develop rapid and reliable diagnostic techniques have been undertaken; a single-step reverse transcription-loop-mediated isothermal amplification (RT-LAMP) assay was developed to detect virus in vector mosquitoes (*Aedes aegypti*) using the Flock House Virus (FHV) as a model. The robustness of the RT-LAMP reaction was revealed by its ability to detect FHV from an "all-in-one" template using whole mosquito bodies within 30 min. Furthermore, RT-LAMP identified successfully a mosquito carrying just a single FHV particle, a level easily overlooked in conventional analysis such as plaque forming assays. These observations suggest that RT-LAMP is more reliable and useful for routine diagnosis of vector mosquitoes in regions where the prevalence of vector-borne diseases such as West Nile fever or dengue fever are common.

© 2008 Elsevier B.V. All rights reserved.

## 1. Introduction

Arboviruses (Arthropod-borne viruses) are transmitted to vertebrates through blood-feeding arthropods consequently leading to diseases of major public health importance worldwide. Indeed, certain mosquito-borne viral diseases have become a major international public health concern including dengue whose global prevalence has grown dramatically in recent decades to the point whereby it is now endemic in more than 100 countries spanning the globe. According to WHO reports there are an estimated 200,000 cases of yellow fever corresponding to 30,000 deaths per year. Although yellow fever has never been reported within Asia this region is at risk due to the presence of both appropriate primates and vectors. Japanese encephalitis (JE) is the leading cause of viral encephalitis throughout large parts of Asia. This disease affects mostly infants and children with some 50,000 cases reported annually and a 25–30% mortality rate with a further 30% rate of long-term effects among survivors. Chikungunya is another mosquito-borne viral disease occurring in Africa and Asia, mainly within the Indian subcontinent. However, more recently mosquito vectors of chikungunya have spread to Europe and North America. Cases of expanded vector ranges such as this are likely to be more common as global temperatures increase making identification and monitoring of viral laden vectors more critical.

Mosquitoes are critical vectors in many arboviral transmission cycles thereby making monitoring of vector populations with a prevalence of arboviruses an important component of risk assessment to humans and animals. Through surveillance of mosquitoes infected with a particular virus, infection rates within the vector mosquito populations harboring a specific virus can provide an early warning sign of an impending epidemic (Samuel and Tyagi, 2006).

Surveillance of vectors for the presence of arbovirus infections often requires pooling of insects due to the low viral infection rate contained with a large mosquito population in endemic areas. Because of this, assays that monitor vector infection rates should ideally be sensitive enough to detect just a single infected mosquito from a large pool. Various types of diagnostic methods aimed at arbovirus detection have been reported including the polymerase chain reaction (PCR) that has been designed to monitor the presence of different viruses within vectors (Chao et al., 2006; Urdaneta et al., 2005; Huang et al., 2001; Wasieloski et al., 1994; Olson et al., 1987). Unfortunately, if the target is a low-copy gene, PCR is

* Corresponding authors. Tel.: +81 155 49 5645; fax: +81 155 49 5643.
E-mail addresses: fukumoto@obihiro.ac.jp (S. Fukumoto), kanuka@obihiro.ac.jp (H. Kanuka).

inadequate to amplify this target reliably in clinical samples without recourse to pathogen multiplication in mice. Furthermore, available molecular methods for pathogen detection require elaborate instruments making their use under field conditions not feasible. There is, therefore, a need for a simplified method of amplification and product detection able to compliment available tests and make feasible molecular diagnosis for case detection and confirmation of eradication in regions that are endemic for vector-borne diseases.

The increased incidence of vector-borne arboviral diseases has prompted further efforts to develop rapid and reliable diagnostic techniques for use in the field for detection of pathogens in vectors. Loop-mediated isothermal amplification (LAMP) is a technique of nucleic acid amplification (Notomi et al., 2000) based on *Bst* DNA polymerase-mediated strand displacement. DNA synthesis occurs at isothermal conditions and relatively low temperatures (60–65 °C) so that there is no need for a thermal cycler. This method has been applied recently for diagnosis of several human pathogenic viruses in addition to the rapid identification of microbial infections. Furthermore, LAMP is being used increasingly by various investigators for rapid detection and typing of emerging arthropod-borne diseases such as dengue, West Nile, chikungunya, Japanese encephalitis (Kurosaki et al., 2006; Mekata et al., 2006; Suzuki et al., 2006; Parida et al., 2005; Hadfield et al., 2001). To date, however, no such study has been applied to the detection of pathogens within their vectors. Therefore this study was carried out to develop a reverse transcription (RT)-LAMP method able to detect arthropod-borne viruses within mosquito vectors (*Aedes aegypti*) using the Flock House Virus (FHV) as a model for vector-arbovirus interaction.

## 2. Materials and methods

### 2.1. Virus, cells, and mosquitoes

Flock House Virus (FHV) was obtained from Dr. Yoshihiro Kawaoka (IMS, University of Tokyo), and stored at −80 °C. *Drosophila* S2 cells were maintained at 25 °C under 5% $CO_2$, with regular passaging every 2 days in Schneider's *Drosophila* medium supplemented with 10% fetal bovine serum, 250 mg/ml peptone

and penicillin/streptomycin. Adult *A. aegypti* mosquitoes were fed with 10% sucrose solution and maintained in a 12/12 h light dark photoperiod at 27 °C and 80% relative humidity.

### 2.2. Preparation of FHV infected mosquitoes

For FHV infection, $CO_2$-anasthetized female *A. aegypti* mosquitoes were injected with 69 nl of Schneider's *Drosophila* medium containing the indicated plaque forming units (PFU) of FHV (approximately $10^3$, $10^2$, $10^1$, $10^0$, and $10^{-1}$ PFU/mosquito). Injection was carried out using calibrated pulled glass needles attached to a microinjector (IM-300, Narishige, Tokyo, Japan). Mosquitoes were always injected in the abdomen, close to the junction with the thorax and just ventral to the junction between the ventral and dorsal cuticles. After injection, the mosquitoes were transferred in batches of 20–25 to mesh covered paper cups, fed with 10% sucrose solution and maintained for 14 days. Mosquitoes were collected every 5 days up to 2 weeks and total RNA was extracted as described below.

### 2.3. Extraction of RNA

RNA was extracted using TRIzol (Invitrogen) from a 250 μl suspension of FHV ($2 \times 10^7$ PFU/ml) or homogenized mosquitoes (1–5 insects). 250 μl of suspension was mixed with 50 μl of PBS and 750 μl of TRIzol reagent and incubated at room temperature for 5 min. 200 μl of chloroform was added and incubated for a further 15 min at room temperature. After centrifugation ($20,400 \times g$, 15 min at 4 °C), 500 μl of supernatant was transferred to a new tube with an equal volume of 2-propanol and incubated for 10 min at room temperature before centrifugation at $20,400 \times g$ for 10 min at 4 °C. The resulting RNA pellet was washed with 70% ethanol, air dried, and dissolved in a minimal volume of TE. RNA solutions were stored at −80 °C.

### 2.4. LAMP primer design

Flock House Virus coat protein precursor alpha gene (GenBank Accession number X15959) was used to design FHV specific primers (Fig. 1). A set of primer was designed for RT-LAMP including two
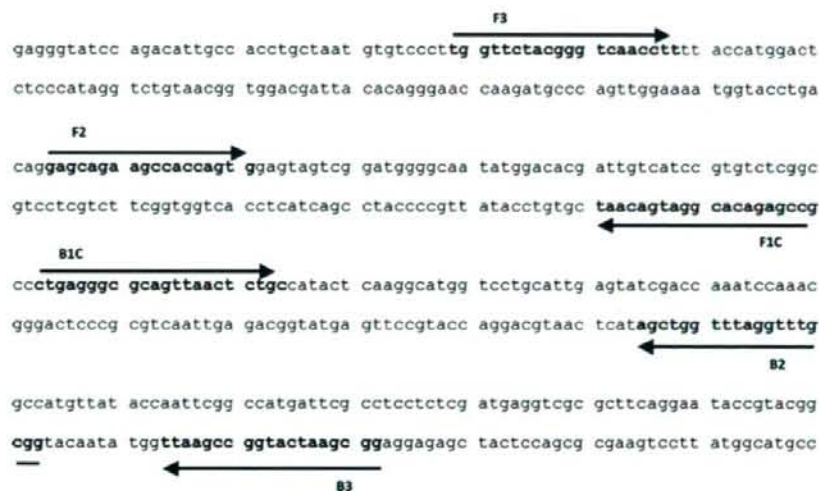


```
                                          F3
gagggtatcc agacattgcc acctgctaat gtgtcccttg gttctacggg tcaacctttt accatggact

ctcccatagg tctgtaacgg tggacgatta cacagggaac caagatgccc agttggaaaa tggtacctga

       F2
caggagcaga agccaccagt ggagtagtcg gatggggcaa tatggacacg attgtcatcc gtgtctcggc

gtcctcgtct tcggtggtca cctcatcagc ctaccccgtt atacctgtgc taacagtagg cacagagccg
                                                                       F1C
    B1C
ccctgagggc gcagttaact ctgccatact caaggcatgg tcctgcattg agtatcgacc aaatccaaac

gggactcccg cgtcaattga gacggtatga gttccgtacc aggacgtaac tcatagctgg tttaggtttg
                                                                    B2
gccatgttat accaattcgg ccatgattcg cctcctctcg atgaggtcgc gcttcaggaa taccgtacgg

cggtacaata tggttaagcc ggtactaagc ggaggagagc tactccagcg cgaagtcctt atggcatgcc
    —
                   B3
```

Fig. 1. Primer design for RT-LAMP in detection of FHV RNA. The sequence of FHV *coat protein precursor alpha* gene from position 791–1061 (GenBank accession number: X15959) was used to design inner and outer primers. Arrows show the location of primer annealing sequence and direction of primer extension.
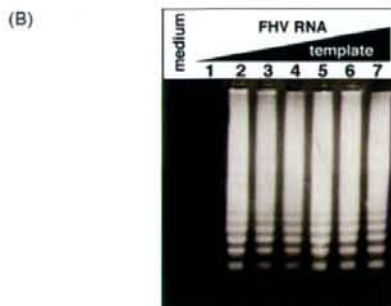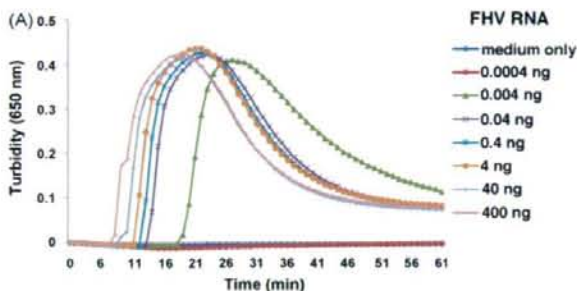
**Table 1**
A primer set designed for the rapid and real time RT-LAMP detection of FHV.

| Primer | Nucleotide sequence (5′–3′) |
|---|---|
| SF16 FHVlamp2F3 | TGGTTCTACGGGTCAACCTT |
| SF16 FHVlamp2B3 | GGCGAATCATGGCCGAATT |
| SF16 FHVlamp2LF | TCCATATTGCCCCATCCGACTACT |
| SF16 FHVlamp2LB | ACTCAAGGCATGGTCCTGCAT |
| SF16 FHVlamp2FIP | CCGAGACACGGATGACAATCGTGAGCAGAAGCCACCAGTG |
| SF16 FHVlamp2BIP | CTGAGGGCGCAGTTAACTCTGCGGCGTTTGGATTTGGTCGA |

**Table 2**
Sensitivity of RT-LAMP for detection of FHV RNA.

| Target RNA concentration of FHV RNA (ng) | Reaction time (min)[a] | Gel electrophoresis |
|---|---|---|
| $4 \times 10^{-4}$ | – | – |
| $4 \times 10^{-3}$ | 20 | + |
| $4 \times 10^{-2}$ | 14 | + |
| $4 \times 10^{-1}$ | 13 | + |
| $4 \times 10^{0}$ | 12 | + |
| $4 \times 10^{1}$ | 10 | + |
| $4 \times 10^{2}$ | 8 | + |

[a] Minimum time before appearance of positive results.

outer primers (F3 and B3), two loop primers (LF and LB), and two inner primers (FIP and BIP) all listed in Table 1. All primers were designed using the LAMP primer design support software program Primer Explorer version 4 (Net Laboratory, Tokyo, Japan; http://primerexplorer.jp/e/).

### 2.5. RT-LAMP

RT-LAMP was carried out using a Loopamp RNA amplification kit (Eiken Chemical, Tokyo, Japan) in accordance with the manufacturer's protocol. Briefly, a 12.5 μl reaction mixture containing 40 pmol each of primers FIP and BIP, 20 pmol each of the loop primers LF and LB and 5 pmol each of the outer primers F3 and B3, 6.25 μl of 2× reaction mix (2.8 mM each dNTPs, 40 mM Tris–HCl (pH 8.8), 20 mM KCl, 16 mM MgSO$_4$, 20 mM (NH$_4$)$_2$SO$_4$, 0.2% Tween 20, and 1.6 M Betain), 0.5 μl of enzyme mix (containing *Bst* DNA polymerase and AMV reverse transcriptase), and 2.5 μl of target RNA was incubated at various temperatures for 60 min before heating at 95 °C for 2 min to terminate the reaction. Real time monitor-ing of LAMP was achieved by recording of the optical density at 650 nm using the Loopamp Realtime Turbidimeter (LA-200, Eiken Chemical, Tokyo, Japan). After turbidity measurement, all amplified products were electrophoresed in a 2% agarose gel in TAE buffer. Gels were visualized under UV after ethidium bromide staining.
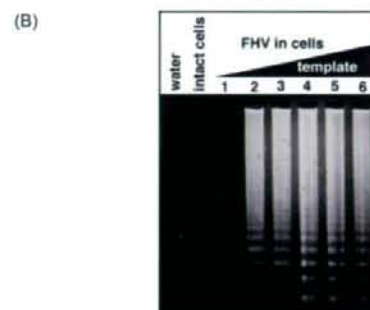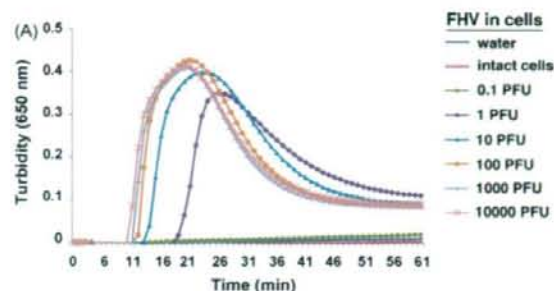
## 3. Results

### 3.1. Sensitivity of RT-LAMP for detection of FHV

Flock House Virus (FHV) is a non-enveloped, positive-sense RNA virus of insect origin belonging to the *Nodaviridae* family and is able to cross the kingdom barrier and replicate in plants, yeast, mammalian cells and insects including *Aedes*, *Culex*, and *Anopheles* mosquitoes (Dasgupta et al., 2003). Also, FHV has been used successfully as an experimental model to study virus-host interactions in a variety of medically important insects (Dasgupta et al., 2007). Primers were designed to target the FHV coat protein precursor alpha gene, taking advantage of the availability of FHV sequence information (Fig. 1 and Table 1). These primers included a set of six primers that examined specificity and sensitivity against coat protein precursor alpha and were initially tested using purified FHV RNA as a template. Sensitivity of detection of FHV was determined via serial 10-fold dilutions of FHV RNA ($4 \times 10^{-4}$ to $4 \times 10^{2}$ ng); at high concentrations, amplified product from $4 \times 10^{2}$ ng of FHV RNA first appeared approximately 8 min after incubation, whereas using 0.4 pg of FHV RNA could not yield a detectable product even 60 min after incubation (Fig. 2A and B and Table 2). In agreement with turbidity analysis, gel electrophoresis confirmed that the RT-LAMP reaction requires at least $4 \times 10^{-3}$ ng of FHV RNA in order to achieve detection thereby determining the lower limits of RT-LAMP detection using this primer set (Fig. 2A and B). Lastly, testing the RT-LAMP at various temperatures (60–67 °C) showed that 63–65 °C to be the optimal incubation temperature for a 60 min reaction (data not shown). These data indicate that the RT-LAMP reaction using the primer set targeting the FHV coat protein precursor alpha gene is able detect purified FHV RNA.

### 3.2. RT-LAMP-based identification of FHV in cultured cells

Detection of FHV in the presence of insect cells was attempted to determine whether cellular components such as proteins, lipids, and nucleic acids might interfere with the RT-LAMP reaction. $5 \times 10^{5}$ *Drosophila* S2 cells were mixed with 10-fold serial dilutions of FHV (0.1–10,000 PFU) that were then subjected to RT-LAMP analysis after total RNA extraction. Both electrophoretic and turbidity analysis indicated that RT-LAMP was able to detect a pool of replicated viruses from just a single PFU of FHV contained within infected cells (Fig. 3A and B).



**Fig. 2.** Sensitivity of RT-LAMP for detection of FHV. (A) Amplification of *coat protein precursor alpha* gene from FHV RNA monitored by real-time turbidimeter (turbidity at 650 nm). Purified FHV RNAs (10-fold serial dilutions from 0.0004 to 400 ng) were used as a template for RT-LAMP reactions for 60 min at 64 °C. An aliquot of medium served as a negative control in RT-LAMP reactions. (B) Agarose-gel electrophoresis of RT-LAMP-amplified products from (A). 1 μl of reaction mixture was electrophoresed on a 2% agarose gel. Amplified DNA showed ladder-like pattern. Lane 1, 0.0004 ng RNA; Lane 2, 0.004 ng RNA; Lane 3, 0.04 ng RNA; Lane 4, 0.4 ng RNA; Lane 5, 4 ng RNA; Lane 6, 40 ng RNA; Lane 7, 400 ng RNA.

**Fig. 3.** RT-LAMP-based identification of FHV in cultured cells. (A) Amplification of *coat protein precursor alpha* gene from FHV in the presence of insect cells monitored by real-time turbidimeter (turbidity at 650 nm). $5 \times 10^5$ *Drosophila* S2 cells were mixed with 10-fold serial dilution of FHV (0.1, 1, 10, 100, 1000, and 10,000 PFU). Total RNA prepared from each solution was used as a template for RT-LAMP reactions for 60 min at 64 °C. An aliquot of water and non-infected cells served as a negative control in RT-LAMP reactions. (B) Agarose-gel electrophoresis of RT-LAMP-amplified products from (A). 1 μl of reaction mixture was electrophoresed on a 2% agarose gel. Amplified DNA showed ladder-like pattern. Lane 1, cells infected with 0.1 PFU FHV; Lane 2, cells infected with 1 PFU FHV; Lane 3, cells infected with 10 PFU FHV; Lane 4, cells infected with 100 PFU FHV; Lane 5, cells infected with 1000 PFU FHV; Lane 6, cells infected with 10,000 PFU FHV.

**Fig. 4.** Evaluation of RT-LAMP for diagnosis of FHV-carrying mosquito. (A) Amplification of *coat protein precursor alpha* gene from FHV-injected mosquitoes monitored by real-time turbidimeter (turbidity at 650 nm). Female *Aedes aegypti* mosquitoes were intrathoracically injected with 10-fold serial dilution of FHV (1, 10, 100, and 1000, PFU/mosquito). Immediately after injection, total RNA prepared from each group (1 mosquito) was used as a template for RT-LAMP reactions for 60 min at 64 °C. Non-injected mosquitoes served as a negative control in RT-LAMP reactions. (B) Agarose-gel electrophoresis of RT-LAMP-amplified products from (A). 1 μl of reaction mixture was electrophoresed on a 2% agarose gel. Amplified DNA showed ladder-like pattern. Lane 1, mosquitoes infected with 1 PFU FHV; Lane 2, mosquitoes infected with 10 PFU FHV; Lane 3, mosquitoes infected with 100 PFU FHV; Lane 4, mosquitoes infected with 1000 PFU FHV.
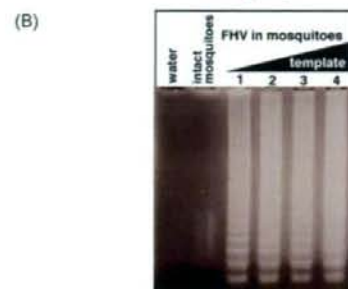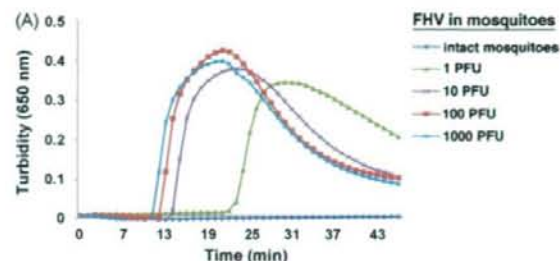
### 3.3. Evaluation of RT-LAMP for diagnosis of FHV-carrying mosquito

It has been demonstrated that mosquitoes carrying even minute amounts of virus are able to transmit infectious pathogens to ver-

**Table 3**
Analysis of RT-LAMP for diagnosis of FHV-carrying mosquito.

| No. of mosquitoes | Day post-infection | PFU/mosquito | | | | | |
|---|---|---|---|---|---|---|---|
| | | 0 | 0.1 | 1 | 10 | 100 | 1000 |
| 1 | 0 | (−) | (−) | (+) | (+) | (+) | (+) |
| | 5 | (−) | (+) | (+) | (+) | (+) | (+) |
| | 10 | (−) | N.D. | (+) | (+) | (+) | (+) |
| | 14 | (−) | (−) | (+) | (+) | (+) | (+) |
| 2 | 0 | (−) | (+) | (+) | (+) | (+) | (+) |
| | 5 | (−) | (+) | (+) | (+) | (+) | (+) |
| | 10 | (−) | N.D. | (+) | (+) | (+) | (+) |
| | 14 | (−) | (−) | (+) | (+) | (+) | (+) |
| 3 | 0 | (−) | (−) | (+) | N.D. | (+) | (+) |
| | 5 | (−) | (+) | (+) | N.D. | N.D. | (+) |
| | 10 | (−) | N.D. | (+) | N.D. | N.D. | (+) |
| | 14 | (−) | (−) | (+) | N.D. | N.D. | (+) |
| 5 | 0 | (−) | (−) | (+) | N.D. | N.D. | (+) |
| | 5 | (−) | (+) | (+) | N.D. | N.D. | (+) |
| | 10 | (−) | N.D. | (+) | N.D. | N.D. | (+) |
| | 14 | (−) | (−) | (+) | N.D. | N.D. | (+) |

N.D., results were not determined.

tebrate hosts during blood feeding. This implies that all mosquitoes harboring viruses need to be identified unfailingly by LAMP in order to ensure a precise and practical survey of potentially infectious regions. To evaluate whether LAMP is sufficient for the diagnosis of virus in mosquitoes, attempts were made to identify experimentally FHV-carrying mosquitoes. Female *A. aegypti* mosquitoes were injected intrathoracically with various concentrations of FHV ($10^{-1}$ to $10^3$ PFU/mosquito) which were then incubated for 14 days, sampling every 4–5 days. Total RNA prepared from these mosquitoes was subjected to RT-LAMP. Concentrations down to $10^{-1}$ PFU/mosquito gave positive responses at the every stage of infection (Table 3) suggesting that the minimum concentration of virus able to be detected was approximately 1 PFU/mosquito (Table 3, Fig. 4A and B). With such high sensitivity and reliability, the LAMP system for diagnosis of FHV-carrying mosquitoes holds promise for field surveys of vector capacity in regions where vector-borne arbovirus diseases are endemic.

## 4. Discussion

Testing mosquito vectors for the presence of human pathogenic viruses could serve as a primary source of arbovirus surveillance data that includes the measurement of mosquito population densities and virus infection rates. Such information has the potential for profound impact for the control and prevention of arboviral diseases and for future epidemiological studies. Consequently it is essential that methods employed in such studies should possess high sensitivity and specificity.

Previously, several techniques have been described on the application of RT-LAMP assays for detection of various types of pathogenic viruses in human and animal samples. Parida et al. (2006) reported the use of RT-LAMP for the analysis of dengue virus serotypes in human serum while Torinawa and Komiya (2006) demonstrated a simple and rapid RT-LAMP method for detection and quantification of Japanese encephalitis virus within infected cell cultures. Several other studies applied RT-LAMP to other RNA viruses such as Ebola virus, (Kurosaki et al., 2006), chikungunya virus, (Parida et al., 2006) as well as DNA viruses such as cytomegalovirus (Suzuki et al., 2006) and Newcastle disease virus (Pham et al., 2005) in clinical samples. However, the application of LAMP to viral detection within arthropod vectors has not been described.

Many previous studies have used various PCR methods, including RT-PCR, nested PCR, and real time PCR for the detection of viruses in mosquitoes (Hadfield et al., 2001; Ibrahim et al., 1996). While these reports have been successful, the use of LAMP took less than 20 min to detect FHV within mosquitoes, much shorter than conventional methods such as PCR and ELISA. Indeed, the standard RT-PCR protocol including reverse transcription, cDNA amplification and detection requires more than 1 h. Furthermore, in terms of PCR-related methods, a thermal cycler is required to carry out DNA amplification whereas the isothermal LAMP method obviates the need for any such equipment. Considering the optimal temperature for FHV detection was determined to be between 63 and 65 °C only a water bath or a heating block would be required to carry out reactions, significant for developing countries where many arboviruses are endemic.

The LAMP reaction can be achieved using six primers thus providing a higher specificity to the reaction than conventional PCR methods. One of the main drawbacks of conventional PCR methods is the inhibition of the reaction by mosquito debris and other biological components (Siridewa et al., 1996), however, it has been reported that LAMP reactions are resistant to such inhibitory materials (Kaneko et al., 2007) consistent with the observation of successful RT-LAMP detection of FHV from a mixture of mosquito debris and DNA. Another advantage of using LAMP is based on the fact that the amplification from stem-loop structures leads to the accumulation of large amounts of products of various lengths, ultimately making detection of amplified DNA much easier including the by-product of the reaction, magnesium pyrophosphate, a white-colored precipitate seen easily by the naked eye (Mori et al., 2001). Thus, these features of the LAMP reaction would be of value especially in emergency cases such as the management of an outbreak of viral diseases.

In conclusion, the RT-LAMP developed is sufficiently sensitive and specific for the identification of FHV within arthropod cells and vectors. Similar RT-LAMP assays could be established for rapid detection of other human pathogenic viruses such as dengue, chikungunya, and Japanese encephalitis, within their vector mosquitoes. In addition, because this assay is simple and does not require sophisticated equipment it can be used potentially as a field method for surveillance of virus-transmitting vectors.

## Acknowledgments

## References

Chao, D.Y., Davis, B.S., Chang, G.J., 2006. Development of multiplex real-time reverse transcriptase PCR assays for detecting eight medically important flaviviruses in mosquitoes. J. Clin. Microbiol. 45, 584–589.

Dasgupta, R., Cheng, L.L., Bartholomay, L.C., Christensen, B.M., 2003. Flock house virus replicates and expresses green fluorescent protein in mosquitoes. J. Gen. Virol. 84, 1789–1797.

Dasgupta, R., Free, H.M., Zietlow, S.L., Paskewitz, S.M., Aksoy, S., Shi, L., Fuchs, J., Hu, C., Christensen, B.M., 2007. Relation of flock House Virus in three genera of medically important insects. J. Med. Entomol. 44, 102–110.

Hadfield, T.L., Turell, M., Dempsey, M.P., David, J., Park, E.J., 2001. Detection of West Nile virus in mosquitoes by RT-PCR. Mol. Cell. Probes 15, 147–150.

Huang, C., Slater, B., Campbell, W., Howard, J., White, D., 2001. Detection of arboviral RNA directly from mosquito homogenates by reverse-transcription-polymerase chain reaction. J. Virol. Methods 94, 121–128.

Ibrahim, M.S., Turell, M.J., Knauert, F.K., Lofts, R.S., 1996. Detection of Rift Valley fever virus in mosquitoes by RT-PCR. Mol. Cell. Probes 11, 49–53.

Kaneko, H., Kawana, T., Fukushima, E., Suzutani, T., 2007. Tolerance of loop-mediated isothermal amplification to a culture medium and biological substances. J. Biochem. Biophys. Methods 70, 499–501.

Kurosaki, Y., Takada, A., Ebihara, H., Grolla, A., Kamo, N., Feldmann, H., Kawaoka, Y., Yasuda, J., 2006. Rapid and simple detection of Ebola virus by reverse transcription-loop-mediated isothermal amplification. J. Virol. Methods 141, 78–83.

Mekata, T., Kono, T., Savan, R., Sakai, M., Kasornchandra, J., Yoshida, T., Itami, T., 2006. Detection of yellow head virus in shrimp by loop-mediated isothermal amplification (LAMP). J. Virol. Methods 135, 151–156.

Mori, Y., Nagamine, K., Tomita, N., Notomi, T., 2001. Detection of loop-mediated isothermal amplification reaction by turbidity derived from magnesium pyrophosphate formation. Biochem. Biophys. Res. Commun. 289, 150–154.

Notomi, T., Okayama, H., Masubuchi, H., Yonekawa, T., Watanabe, K., Amino, N., Hase, T., 2000. Loop-mediated isothermal amplification of DNA. Nucleic Acids Res. 28, e63.

Olson, K., Blair, C., Padmanabhan, R., Beaty, B., 1987. Detection of dengue virus type 2 in Aedes albopictus by nucleic acid hybridization with strand-specific RNA probes. J. Clin. Microbiol. 26, 579–581.

Parida, M., Horioke, K., Ishida, H., Dash, P.K., Saxena, P., Jana, A.M., Islam, M.A., Inoue, S., Hosaka, N., Morita, K., 2005. Rapid detection and differentiation of dengue virus serotypes by a real-time reverse transcription-loop-mediated isothermal amplification assay. J. Clin. Microbiol. 43, 2895–2903.

Parida, M.M., Santhosh, S.R., Dash, P.K., Tripathi, N.K., Lakshmi, V., Mamidi, N., Shrivastva, A., Gupta, N., Saxsena, P., Babu, J.P., Rao, P.V.L., Morita, K., 2006. Rapid and real time detection of chikungunya virus by reverse transcription loop-mediated isothermal amplification assay. J. Clin. Microbiol. 45, 351–357.

Pham, H.M., Nakajima, C., Ohashi, K., Onuma, M., 2005. Loop-mediated isothermal amplification for rapid detection of Newcastle disease virus. J. Clin. Microbiol. 43, 1646–1650.

Samuel, P.P., Tyagi, B.K., 2006. Diagnostic methods for detection & isolation of dengue viruses from vector mosquitoes. Indian J. Med. Res. 123, 615–628.

Siridewa, K., Karunanayake, E.H., Chandrasekaran, N.V., 1996. Polymerase chain reaction-based technique for the detection of Wuchereria bancrofti in human blood samples, hydrocele fluid, and mosquito vectors. Am. J. Trop. Med. Hyg. 54, 72–76.

Suzuki, R., Yoshikawa, T., Ihira, M., Enomoto, Y., Inagaki, S., Matsumoto, K., Kato, K., Kudo, K., Kojima, S., Asano, Y., 2006. Development of the loop-mediated isothermal amplification method for rapid detection of cytomegalovirus DNA. J. Virol. Methods 132, 216–221.

Torinawa, H., Komiya, T., 2006. Rapid detection and quantification of Japanese encephalitis virus by real-time reverse transcription loop-mediated isothermal amplification. Microbiol. Immunol. 50, 379–387.

Urdaneta, L., Herrera, F., Pernalete, M., Zoghbi, N., Palis, Y.R., Barrios, R., Rivero, J., Comach, G., Jimenes, M., Salcedo, M., 2005. Detection of dengue viruses in field-caught Aedes aegypti (Diptera: Culcidae) in Maracay, Aragua state, Venezuela by type-specific polymerase chain reaction. Infect. Genet. Evol. 5, 177–184.

Wasieloski, L., Keller, A.R., Curtis, L.A., Blair, C.D., Beaty, B.J., 1994. Reverse transcription-PCR detection of Lacrosse virus in mosquitoes and comparison with enzyme immunoassay and virus isolation. J. Clin. Microbiol. 32, 2076–2080.

Contents lists available at ScienceDirect

## Biochemical and Biophysical Research Communications

journal homepage: www.elsevier.com/locate/ybbrc

# Rapid identification of *Plasmodium*-carrying mosquitoes using loop-mediated isothermal amplification

Hiroka Aonuma [a,b], Moemi Suzuki [a], Hiroshi Iseki [a], Namal Perera [a], Bryce Nelson [a], Ikuo Igarashi [a], Takeshi Yagi [b], Hirotaka Kanuka [a,*], Shinya Fukumoto [a,*]

[a] National Research Center for Protozoan Diseases, Obihiro University of Agriculture and Veterinary Medicine, Inada-cho, Obihiro, Hokkaido 080-8555, Japan
[b] KOKORO Biology Group, Laboratories for Integrated Biology, Graduate School of Frontier Biosciences, Osaka University, Suita, Osaka 565-0871, Japan

### ABSTRACT

With an aim to develop a quick and simple method to survey pathogen-transmitting vectors, LAMP (loop-mediated isothermal amplification) was applied to the identification of *Plasmodium*-carrying mosquitoes, specifically a *Plasmodium*-transmitting experimental model using rodent malaria parasite (*Plasmodium berghei*) and anopheline mosquitoes (*Anopheles stephensi*). The detection sensitivity limit of the LAMP reaction amplifying the SPECT2 gene was determined to be $1 \times 10^2$ purified *Plasmodium* parasites, estimated to be sufficient for reliable identification of infectious mosquitoes. The robustness of the LAMP reaction was revealed by its ability to detect both *Plasmodium* oocysts and sporozoites from an "all-in-one" template using whole mosquito bodies. Moreover, LAMP successfully identified an infectious mosquito carrying just a single oocyst in its midgut, a level that can be easily overlooked in conventional microscopic analysis. These observations suggest that LAMP is more reliable and useful for routine diagnosis of vector mosquitoes in regions where vector-borne diseases such as malaria are endemic.

© 2008 Elsevier Inc. All rights reserved.

Malaria is a major life-threatening disease causing at least 1 million deaths every year in the world [1] and is caused by a protozoan parasite, *Plasmodium* subspecies, transmitted via the vector anopheline mosquitoes. To control these malaria-transmitting vectors, precise surveillance data of *Plasmodium*-carrying mosquitoes antecedent to implementation of countermeasures is crucial [2]. *Plasmodium* begins its development in the anopheline mosquito immediately after the female sucks blood meal from infected vertebrate hosts, subsequently drawing in the *Plasmodium* gametocytes. Within the mosquito midgut, the male gametocyte undergoes rapid nuclear divisions, producing flagellated microgametes that are able to fertilize the female macrogamete. The resulting zygotic ookinete traverses the mosquito gut wall and encysts on the exterior of the gut wall to form an oocyst. Soon the oocyst ruptures, releasing hundreds of sporozoites into the mosquito body cavity where they eventually migrate to the mosquito salivary gland. Since even 1–10 sporozoites are capable of causing malaria in host animals following invasion into the blood stream after blood feeding [3], an ideal diagnostic method should have a lower limit of only a single *Plasmodium* oocyst or sporozoite in mosquitoes in order to be able to garner precise information of both disease prevalence and vectorial capacity.

Microscopic analysis has been the most commonly used method for diagnosis of *Plasmodium* in both humans and mosquitoes and is still considered as the most reliable standard. However, microscopic detection of *Plasmodium* requires a trained-eye and in the case of blood smears, the detection sensitivity limit of microscopic examination has been estimated to be 5 parasites in 1 microliter of blood sample [4], a level that is reached after patients become symptomatic [5,6]. Similarly, *Plasmodium* levels in mosquitoes have also often been underestimated during examination of infection rates of mosquitoes [7]. Recently, polymerase chain reaction (PCR) has been employed as a more reliable method for diagnosis of *Plasmodium*; detection of *Plasmodium* in mosquito salivary gland by PCR is three times more sensitive than microscopic examination [7]. However, PCR is known to be temperamental with easily terminated reactions dependent on the condition of samples and reagents, particularly in relation to contamination of debris from host or vector cells. Using blood samples in filter paper from *Plasmodium*-infected patients, a previous work observed that PCR detected only 73% of positive samples and often failed to capture less than 200 parasites in 1 μl of blood sample [8]. Recently ELISA has also been used for diagnosis and been shown to be able to detect relatively low *Plasmodium* density to a level as low as 12 asexual parasites in 1 microliter of blood [9]. However, despite the sensitivity, ELISA is laborious and time-consuming particularly when handling large numbers of samples. Therefore, in order to improve on surveillance methods for *Plasmodium*-carrying

---

* Corresponding authors. Fax: +81 155 49 5643 (H. Kanuka).
  *E-mail addresses:* kanuka@obihiro.ac.jp (H. Kanuka), fukumoto@obihiro.ac.jp (S. Fukumoto).

mosquitoes, a novel, quick and simple method should be applied. In addition to ease, the sensitivity of the novel method should be high enough to identify all infectious mosquitoes. With these points in mind, we propose a novel surveillance strategy that is simpler and quicker than previous methods, in addition to being as sensitive and reliable as PCR or ELISA.

LAMP (loop-mediated isothermal amplification) is a novel DNA amplification method with the distinguished feature that the reaction can proceed under isothermal conditions [10]; the LAMP reaction requires only a single enzyme, *Bst* DNA polymerase that can synthesize a new strand of DNA while simultaneously displacing the former complementary strand thereby enabling DNA amplification at a single temperature. The LAMP reaction can be achieved using four primers (FIP, BIP, F3, and B3), two of which (F3 and B3) contribute to the formation of a stem-loop structure while the other two (FIP and BIP), designed complementary to the inner sequence of the stem-loop structure, are employed for amplification of the target sequence, thus providing a higher specificity to the reaction than conventional PCR methods. Another advantage using LAMP is based on the fact that the amplification from stem-loop structures leads to the accumulation of large amounts of products of various lengths, ultimately making detection of amplified DNA much easier. Furthermore, the by-product of the reaction, magnesium pyrophosphate, is a white-colored precipitate easily seen by the naked eye [11]. Taken together, these features suggest LAMP as an appropriate diagnostic method to survey pathogen-carrying mosquito populations essential for effective disease-controlling measures. In this study, we applied LAMP to the detection of the malaria parasite, *Plasmodium*, within the anopheline mosquito and elucidated its usefulness and reliability thereby demonstrating its potential as an important diagnostic tool to be coupled with classic malaria control measures.

## Materials and methods

*Preparation of parasites and infected mosquitoes.* BALB/c mice (7–8 week) were infected with rodent malaria parasite, *Plasmodium berghei* ANKA strain (containing GFP driven by the *hsp70* promoter for easy visualization, a gift from Dr. M. Yuda [12]) by injection of infected blood. Female *Anopheles stephensi* were then allowed to feed on anaesthetized infected BALB/c mice. Mosquitoes were kept at 19 °C after feeding until dissection for microscopic analysis or sporozoite preparation, 22–24 days post feeding in the case of salivary sporozoite collection. Salivary glands removed from mosquitoes were collected in M199 media (Sigma) on ice and ground gently with a plastic homogenizer to release sporozoites that were subsequently collected from the supernatant after centrifugation at 500 rpm, 4 °C. For evaluation of LAMP using oocyst-carrying mosquitoes, each mosquito midgut was dissected in ice-cold PBS and microscopically analyzed to count the number of oocysts before collection and storage at −20 °C of midguts along with the carcasses in the same tube until DNA extraction.
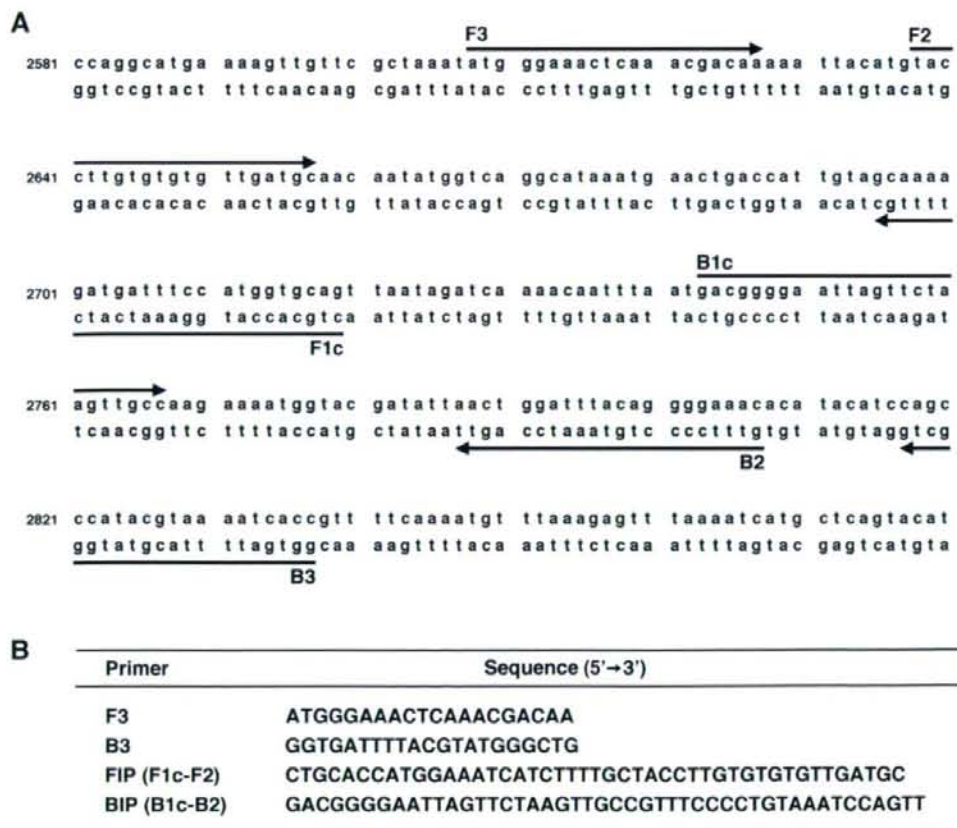


**Fig. 1.** LAMP primer set targeting *P. berghei SPECT2*. (A) Partial sequence of *P. berghei SPECT2* and location of primers, FIP (F1c-F2), BIP (B1c-B2), F3, and B3. Arrows indicate sequences of primers and directions of extensions. Numbers on the left indicate the nucleotide position. (B) Sequence of primers for LAMP reaction.

*DNA extraction.* Genomic DNA of *P. berghei*-infected red blood cells, *Plasmodium* sporozoites, and infected mosquitoes was extracted as follows: infected red blood cells, sporozoites, and infected mosquitoes were collected and homogenized with a plastic homogenizer in 100 µl of Buffer A (0.1 M Tris (pH 9.0), 0.1 M EDTA, 1% SDS, and 0.5% DEPC), and incubated for 30 min at 70 °C. 22.4 µl of 5 M KoAc was added to the mixture and incubated for 30 min on ice. Supernatant was collected by centrifugation at 15,000 rpm for 15 min at 4 °C, and mixed with 45 µl of isopropanol. Precipitated DNA was collected after centrifugation at 15,000 rpm for 20 min at 4 °C, rinsed with 70% ethanol, and dried. Each DNA pellet was diluted in TE to achieve a concentration such that 1 µl of solution would contain DNA from $1 \times 10^5$ infected red blood cells, $1 \times 10^4$ sporozoites, or one-fifth of a mosquito. One microliter of each DNA solution was then used as a template for the LAMP reaction.

*LAMP reactions.* The specific primers for LAMP reaction were designed against the *P. berghei SPECT2* gene [13]. The locus and sequence of each primer (F3, B3, FIP, BIP) in this gene are described in Fig. 1. The LAMP reaction was performed as manufacture's instructions (Eiken Chemical Co., Ltd., Tokyo, Japan). Briefly, the reaction was performed in 12.5 µl of reaction mixture containing 1 µl of extracted DNA solution, 2.5 pmol of each F3 and B3 primers, 20 pmol of each FIP and BIP primers, 6.25 µl of 2× reaction mixture, and 0.5 µl of *Bst* DNA polymerase. The reaction mixture was incubated at 59 °C for 75 min using a Loopamp Realtime Turbidimeter (LA-200; Eiken Chemical Co., Ltd., Tokyo, Japan) and terminated by incubation at 95 °C for 2 min.

*Analysis of LAMP products.* Amplified DNA in the LAMP reaction causes turbidity due to the accumulation of magnesium pyrophosphate, a by-product of the reaction. Turbidity was monitored using Loopamp Realtime Turbidimeter (LA-200; Eiken Chemical Co., Ltd., Tokyo, Japan), and also observed by the naked eye. All LAMP products were electrophoresed in 2% agarose gels, stained with ethidium bromide and visualized under UV light.

## Results

### Sensitivity of LAMP for detection of P. berghei.

Primers were designed to target the *P. berghei SPECT2* gene, taking advantage of the availability of *P. berghei* sequence information [13] (Fig. 1). These primers included a set of four primers that examined specificity and sensitivity against *SPECT2* using *P. berghei*-infected red blood cells as a template. Initial tests of this primer set were performed using serial dilutions of *P. berghei* DNA prepared from infected red blood cells and indicated that LAMP reactions can detect parasite DNA collected down to a level of just $1 \times 10^2$ of red blood cells infected with *P. berghei* (data not shown), consistent with previous studies detecting *P. falciparum* and *P. vivax* by LAMP [14]. The optimized LAMP reaction conditions of temperature and time using the primer set were 59 °C and 75 min, respectively (data not shown). These experiments were repeated three times for verification.

Having determined the experimental conditions, the sensitivity of LAMP reactions in the detection of the *P. berghei* parasite contained within a vector was then elucidated. *P. berghei* sporozoite DNA (equivalent to $1 \times 10^0$, $1 \times 10^1$, $1 \times 10^2$, $1 \times 10^3$, and $1 \times 10^4$ parasites) collected from infected mosquitoes was used as template for LAMP reactions. Under the same conditions (75 min at 59 °C) the amplified product from the DNA of $1 \times 10^4$ sporozites first appeared at approximately 40 min after incubation, whereas 1–10 parasites could not be detected even after 75 min incubation (Fig. 2A). In agreement with turbidity analysis, gel electrophoresis revealed that the LAMP reaction requires at least $1 \times 10^2$ sporozoites in order to achieve detection thereby determining the lower
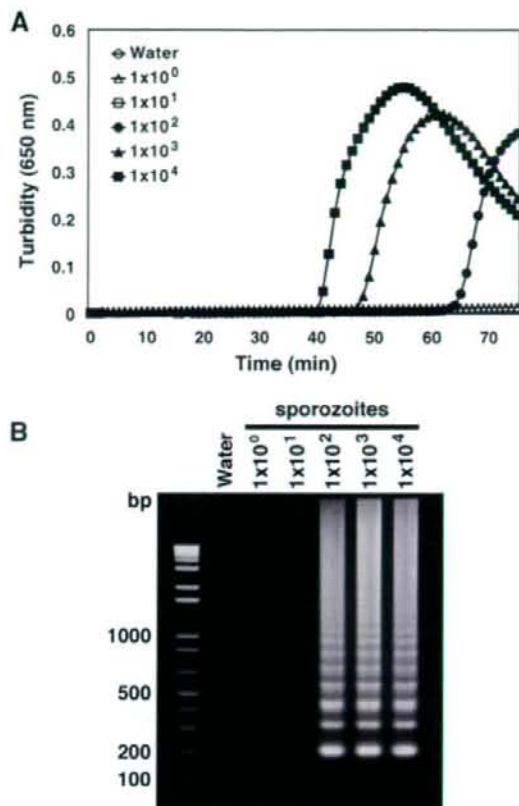


Fig. 2. Sensitivity of LAMP for detection of *P. berghei*. (A) Amplification of *SPECT2* from *Plasmodium* sporozoite with primer set monitored by real-time turbidimeter (turbidity at 650 nm). *P. berghei* sporozoite DNA (equivalent to $1 \times 10^0$, $1 \times 10^1$, $1 \times 10^2$, $1 \times 10^3$, and $1 \times 10^4$ parasites) was used as a template for LAMP reactions for 75 min at 59 °C. An aliquot of water served as a negative template in LAMP reaction. (B) Agarose-gel electrophoresis of LAMP-amplified products from (A). One microliter of reaction mixture was electrophoresed on 2% agarose gel. Numbers on the left indicate migration of molecular weight marker (100 bp + 1 kb DNA ladder).

limits of LAMP detection, using this primer set of *P. berghei* (Fig. 2B). These data indicate that the LAMP reaction using the primer set targeting the *P. berghei SPECT2* gene is able to detect purified parasites collected from both the blood and vector stage. In terms of sensitivity of this LAMP reaction, this method is sufficient for detection of infectious mosquitoes that typically hold more than $10^4$ sporozoites within their salivary glands [15].

### LAMP-based identification of P. berghei-carrying mosquito

To evaluate whether the LAMP method is appropriate for diagnosis of pathogen-carrying mosquitoes, we attempted to experimentally identify *Plasmodium*-carrying mosquitoes among an intact mosquito population. Approximately 200 female mosquitoes (*Anopheles stephensi*) were allowed to simultaneously feed on a single BALB/c mouse infected with GFP-expressing transgenic *P. berghei*. GFP-expressing *P. berghei* have been shown to provide facile and reliable microscopic analysis of infection [16,17]. Time was limited in order to ensure a mixed population of fed and non-fed mosquitoes that were then incubated for 16 days before collection to allow time for oocyst and sporozoite development. A number of mosquitoes were randomly sampled for further examination. Prior

to DNA extraction, each mosquito was examined microscopically, using GFP fluorescence as an indication of *P. berghei* infection and development. Some mosquitoes showed robust GFP signal in their abdomen and neck indicating they were carrying large numbers of oocysts and sporozoites (Fig. 3A, C, and D). One mosquito exhibited a weak but significant GFP signal in its abdomen suggesting a small number of oocysts (Fig. 3G), while no signal could be detected in the remaining mosquitoes (Fig. 3B, E, and F). Each of these mosquitoes was then subjected to LAMP analysis. Both electrophoretic and turbidity analysis provided results consistent with microscopic analysis: all mosquitoes carrying *Plasmodium* parasites were identified as positive via the LAMP-based diagnosis (Fig. 3H and I).

*Evaluation of LAMP for diagnosis of P. berghei-carrying mosquito*

It has been demonstrated that mosquitoes carrying just a single midgut oocyst are able to transmit infectious sporozoites to vertebrate hosts during blood feeding. This implies that all mosquitoes containing more than one oocyst need to be identified unfailingly by LAMP in order to ensure a precise and practical survey of potentially infectious regions. To evaluate usability of the LAMP method as a practical vector-diagnostic method, LAMP-based detection of *P. berghei* in mosquito was carried out in more detail. Mosquitoes were dissected for microscopic analysis in order to count maturing oocysts 8 days after sucking blood infected with GFP-expressing transgenic *P. berghei*. In an experiment using 6 independent mosquito samples, the number of oocysts ranged from 1 to 367 (Fig. 4A–F). After microscopic observation, each analyzed midgut was collected together with its carcass before being subjected to DNA extraction to be used as a template for LAMP reactions. Again, the amplified product

of each reaction mixture was determined by both electrophoresis and a real-time turbidimeter, revealing a detection profile significantly correlated with oocyst numbers (Fig. 4G and H). It is particularly worth noting that even just a single oocyst contained within a mosquito could be successfully detected by the LAMP reaction (Fig. 4G).

**Discussions**

Vector control is an essential component of programs designed to manage a worsening malaria situation around the world [2]. Precise survey data is the basis of decision-making that can enormously increase the effectiveness of insecticide-based control. Furthermore, accurate survey reduces inappropriate use of insecticides and resources. Despite its importance, use of available new strategies for pathogen-carrying vector survey has been clearly undervalued and microscopic analysis remains the standard technique. Still, a novel method is demanded for rapid and precise surveillance of infectious mosquitoes in malaria-endemic areas. A method for diagnosis that can be simple enough to avoid extensive training is necessary as well as fast enough to process hundreds of mosquitoes per day by a single person plus be more reliable than previously used methods.

In the present study, we have demonstrated the usefulness of LAMP for the surveillance of infectious mosquitoes. *Plasmodium* DNA was successfully amplified and detected by the LAMP reaction even in a condition containing copious amounts of contaminating DNA from the debris of mosquitoes. When nearly pure DNA from *Plasmodium* sporozoites was used, the detection limit for *Plasmodium* sporozoites was 100 sporozoites in 1 microliter (Fig. 2). In terms of sensitivity of this LAMP reaction, one infected mosquito often carries as many as $10^4$ sporozoites in their salivary glands
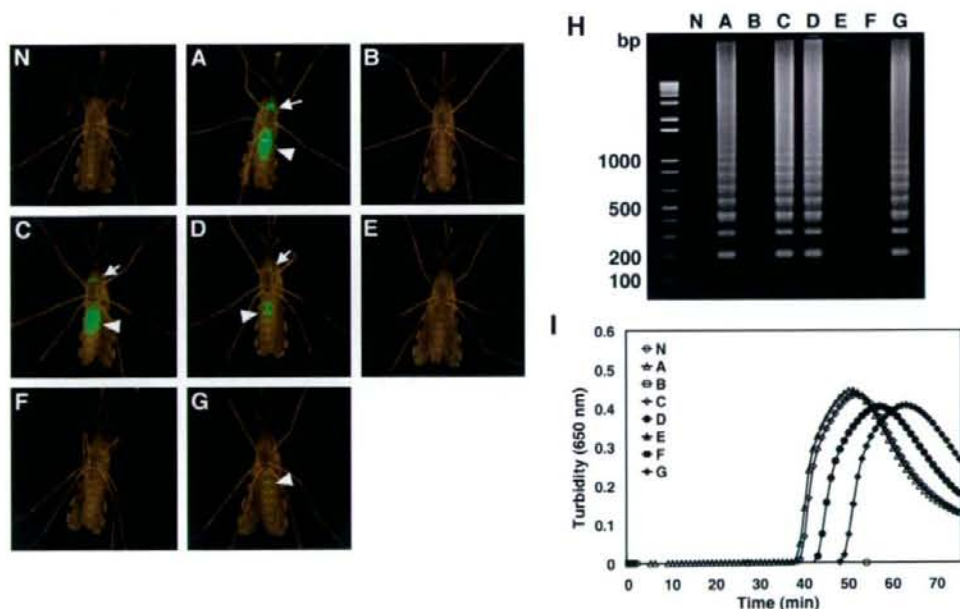


**Fig. 3.** LAMP-based identification of *P. berghei*-carrying mosquito. (A–G) Randomly selected mosquitoes from a population containing both fed and unfed female mosquitoes. Each mosquito was observed for its infection state under fluorescent microscopy. GFP signal (green spots) indicates oocysts in mosquito midgut (around abdomen: white arrowhead) and sporozoites in salivary gland (around neck: white arrow). An uninfected mosquito shown in (N) was used as negative control. (H,I) LAMP detection of *P. berghei* in each mosquito by electrophoresis (H) and real-time turbidimeter (I). Mosquito DNA samples containing *P. berghei* DNA corresponding to (N)–(G) were used as templates in the LAMP reaction for 75 min at 59 °C. *P. berghei* DNA from infected red blood cells was used as positive control (R). One microliter of reaction mixture was electrophoresed on a 2% agarose gel. Numbers on the left in (H) indicate migration of molecular weight marker (100 bp + 1 kb DNA ladder).
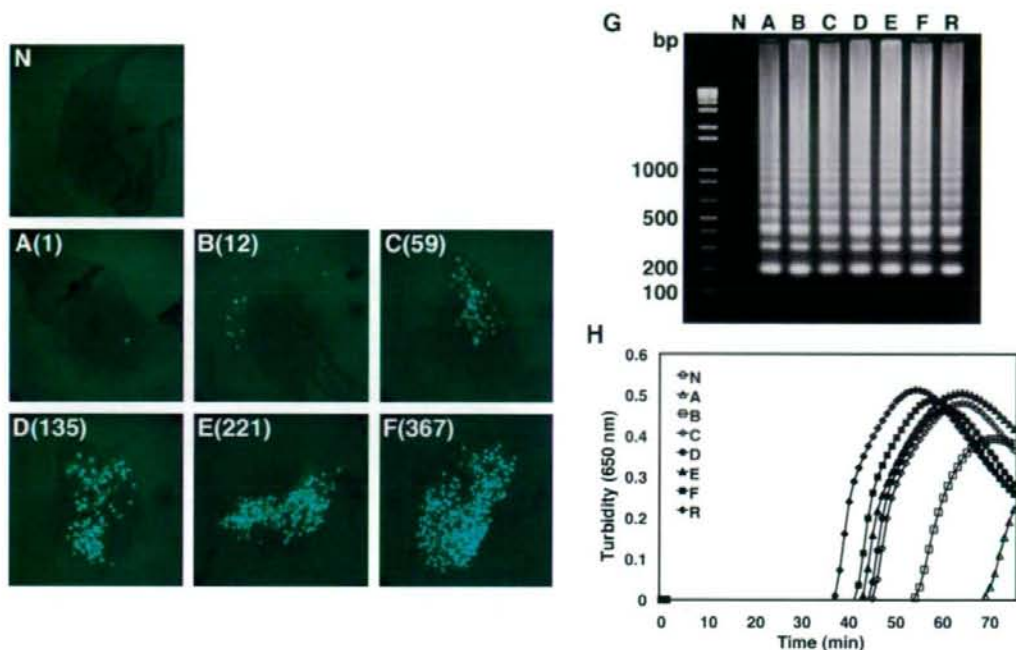
Fig. 4. Evaluation of LAMP for diagnosis of *P. berghei*-carrying mosquito. (A–F) Mosquito midgut containing *P. berghei* oocysts. *P. berghei* oocysts expressing GFP in mosquitoes were counted under fluorescent microscopy prior to LAMP analysis. Numbers in panels (parentheses) indicate the number of oocysts in midgut shown as GFP signal (green). A midgut of uninfected mosquito shown in (N) was used as a negative control. (G,H) LAMP detection of *P. berghei* oocysts in each mosquito by electrophoresis (G) and real-time turbidimeter (H). Mosquito DNA samples containing *P. berghei* DNA corresponding to (N)–(F) were used as templates in the LAMP reaction for 75 min at 59 °C. *P. berghei* DNA from infected red blood cells was used as positive control (R). One microliter of reaction mixture was electrophoresed on a 2% agarose gel. Numbers on the left in (G) indicate migration of molecular weight marker (100 bp + 1 kb DNA ladder).

and inject 15–80 sporozoites when causing malaria disease in humans during blood feeding [15], suggesting that this method is abundantly sufficient at identifying infectious mosquitoes. Furthermore, the applicability of LAMP for the diagnosis of infectious mosquitoes was successfully demonstrated upon detection of *Plasmodium* oocysts or sporozoites in infected mosquitoes (Figs. 3 and 4). Comparison of accuracy of microscopic analysis and LAMP revealed higher reliability in LAMP; even just a single oocyst, which is likely to be overlooked by standard microscopy, was detectable by LAMP (Fig. 4).

Even though LAMP has been considered as a novel diagnostic method for various infectious diseases, including the human malaria pathogen *P. falciparum* [14,18,19], most of those studies were aimed at the detection of the pathogen within blood samples from the vertebrate host whereas its application directed towards detection of a pathogen within an arthropod vector has thus far been neglected. However, results in this report suggest that LAMP is likely more suitable for vector diagnosis since the whole body of a parasite-carrying vector can be provided for LAMP-based diagnosis, whereas a larger volume of blood is needed in order to ensure sufficient pathogen numbers to provide a template for a positive reaction from the vertebrate host.

Moreover, due to its isothermal reaction conditions and simple diagnostic output, LAMP could be easily combined with a typical field collection of vectors to survey pathogens *in situ*; indeed, only warm water would be needed to perform this assay. With high sensitivity and reliability of the LAMP system for diagnosis of *Plasmodium*-carrying mosquitoes, this method holds great promise to achieve useful field surveys of vectorial capacity in regions where malaria is endemic.

## References

[1] WHO, Fact sheet N°94, World Health Organization, 2007.
[2] WHO, Vector control for malaria and other mosquito-borne diseases, WHO technical report series, 857, 1995.
[3] R.E. Sinden, H.M. Gilles, The malaria parasites, in: D.A. Warrell, H.M. Gilles (Eds.), Essential Malariology, Arnold, London, 2002, pp. 8–34.
[4] R.H. Barker Jr, T. Banchongaksorn, J.M. Courval, W. Suwonkerd, K. Rimwungtragoon, D.F. Wirth, A simple method to detect *Plasmodium falciparum* directly from blood samples using the polymerase chain reaction, Am. J. Trop. Med. Hyg. 46 (1992) 416–426.
[5] D.F. Verhage, D.S. Telgt, J.T. Bousema, C.C. Hermsen, G.J. van Gemert, J.W. van der Meer, R.W. Sauerwein, Clinical outcome of experimental human malaria induced by *Plasmodium falciparum*-infected mosquitoes, Neth. J. Med. 63 (2005) 52–58.
[6] J.E. Epstein, S. Rao, F. Williams, D. Freilich, T. Luke, M. Sedegah, P. de la Vega, J. Sacci, T.L. Richie, S.L. Hoffman, Safety and clinical outcome of experimental challenge of human volunteers with *Plasmodium falciparum*-infected mosquitoes: an update, J. Infect. Dis. 196 (2007) 145–154.
[7] M.D. Wilson, A. Ofosu-Okyere, A.U. Okoli, P.J. McCall, G. Snounou, Direct comparison of microscopy and polymerase chain reaction for the detection of

Plasmodium sporozoites in salivary glands of mosquitoes, Trans. R. Soc. Trop. Med. Hyg. 92 (1998) 482–483.

[8] K.K. Scopel, C.J. Fontes, A.C. Nunes, M.F. Horta, E.M. Braga, Low sensitivity of nested PCR using Plasmodium DNA extracted from stained thick blood smears: an epidemiological retrospective study among subjects with low parasitaemia in an endemic area of the Brazilian Amazon region, Malaria J. 3 (2004).

[9] H. Noedl, K. Yingyuen, A. Laoboonchai, M. Fukuda, J. Sirichaisinthop, R.S. Miller, Sensitivity and specificity of an antigen detection ELISA for malaria diagnosis, Am. J. Trop. Med. Hyg. 75 (2006) 1205–1208.

[10] T. Notomi, H. Okayama, H. Masubuchi, T. Yonekawa, K. Watanabe, N. Amino, T. Hase, Loop-mediated isothermal amplification of DNA, Nucleic Acid Res. 28 (2000) E63.

[11] Y. Mori, K. Nagamine, N. Tomita, T. Notomi, Detection of loop-mediated isothermal amplification reaction by turbidity derived from magnesium pyrophosphate formation, Biochem. Biophys. Res. Commun. 289 (2001) 150–154.

[12] T. Ishino, Y. Orito, Y. Chinzei, M. Yuda, A calcium-dependent protein kinase regulates Plasmodium ookinete access to the midgut epithelial cell, Mol. Microbiol. 59 (2006) 1175–1184.

[13] T. Ishino, Y. Chinzei, M. Yuda, A Plasmodium sporozoite protein with a membrane attack complex domain is required for breaching the liver sinusoidal cell layer prior to hepatocyte infection, Cell Microbiol. 7 (2005) 199–208.

[14] E.T. Han, R. Watanabe, J. Sattabongkot, B. Khuntirat, J. Sirichaisinthop, H. Iriko, L. Jin, S. Takeo, T. Tsuboi, Detection of four Plasmodium species by genus- and species-specific loop-mediated isothermal amplification for clinical diagnosis, J. Clin. Microbiol. 45 (2007) 2521–2528.

[15] R.E. Sinden, P.F. Billingsley, Plasmodium invasion of mosquito cells: hawk or dove?, Trends Parasitol. 17 (2001) 209–212.

[16] B. Franke-Fayard, H. Trueman, J. Ramesar, J. Mendoza, M. van der Keur, R. van der Linden, R.E. Sinden, A.P. Waters, C.J. Janse, A Plasmodium berghei reference line that constitutively expresses GFP at a high level throughout the complete life cycle, Mol. Biochem. Parasitol. 137 (2004) 23–33.

[17] S. Blandin, S.H. Shiao, L.F. Moita, C.J. Janse, A.P. Waters, F.C. Kafatos, E.A. Levashina, Complement-like protein TEP1 is a determinant of vectorial capacity in the malaria vector Anopheles gambiae, Cell 116 (2004) 661–670.

[18] L.L. Poon, B.W. Wong, E.H. Ma, K.H. Chan, L.M. Chow, W. Abeyewickreme, N. Tangpukdee, K.Y. Yuen, Y. Guan, S. Looareesuwan, J.S. Peiris, Sensitive and inexpensive molecular test for falciparum malaria: detecting Plasmodium falciparum DNA directly from heat-treated blood by loop-mediated isothermal amplification, Clin. Chem. 52 (2006) 303–306.

[19] D.H. Paris, M. Imwong, A.M. Faiz, M. Hasan, E.B. Yunus, K. Silamut, S.J. Lee, N.P. Day, A.M. Dondorp, Loop-mediated isothermal PCR (LAMP) for the diagnosis of falciparum malaria, Am. J. Trop. Med. Hyg. 77 (2007) 972–976.

# Mitogen-Activated Protein Kinase-Activated Kinase RSK2 Plays a Role in Innate Immune Responses to Influenza Virus Infection[∇]

Satoshi Kakugawa,[1] Masayuki Shimojima,[1] Hideo Goto,[1] Taisuke Horimoto,[1] Naoki Oshimori,[3] Gabriele Neumann,[5] Tadashi Yamamoto,[3] and Yoshihiro Kawaoka[1,2,4,5*]

*Division of Virology, Department of Microbiology and Immunology, Institute of Medical Science, University of Tokyo, 4-6-1 Shirokanedai, Minato-ku, Tokyo 108-8639, Japan[1]; Exploratory Research for Advanced Technology (ERATO), Japan Science and Technology Agency, Saitama 332-0012, Japan[2]; Division of Oncology, Institute of Medical Science, University of Tokyo, 4-6-1 Shirokanedai, Minato-ku, Tokyo 108-8639, Japan[3]; International Research Center for Infectious Diseases, Institute of Medical Science, University of Tokyo, Tokyo 108-8639, Japan[4]; and Department of Pathobiological Sciences, School of Veterinary Medicine, University of Wisconsin, Madison, Wisconsin 53706[5]*

Viral infections induce signaling pathways in mammalian cells that stimulate innate immune responses and affect cellular processes, such as apoptosis, mitosis, and differentiation. Here, we report that the ribosomal protein S6 kinase alpha 3 (RSK2), which is activated through the "classical" mitogen-activated protein kinase pathway, plays a role in innate immune responses to influenza virus infection. RSK2 functions in the regulation of cell growth and differentiation but was not known to play a role in the cellular antiviral response. We have found that knockdown of RSK2 enhanced viral polymerase activity and growth of influenza viruses. Influenza virus infection stimulates NK-κB- and beta interferon-dependent promoters. This stimulation was reduced in RSK2 knockdown cells, suggesting that RSK2 executes its effect through innate immune response pathways. Furthermore, RSK2 knockdown suppressed influenza virus-induced phosphorylation of the double-stranded RNA-activated protein kinase PKR, a known antiviral protein. These findings establish a role for RSK2 in the cellular antiviral response.

Influenza A viruses cause highly contagious respiratory infections in humans and several animal species (reviewed in reference 51). Annual epidemics account for an estimated 20,000 excess deaths and 100,000 excess hospitalizations in the United States alone. Pandemics occur at irregular intervals and can claim millions of lives, as witnessed with the "Spanish influenza" in 1918 and 1919, which killed an estimated 40 to 50 million people worldwide.

Influenza A viruses belong to the family *Orthomyxoviridae* and possess eight segments of single-stranded, negative-sense RNA, which encode 10 or 11 proteins (reviewed in reference 36). Four viral proteins—the polymerase subunits PB2, PB1, and PA and the nucleoprotein NP—are required for the replication and transcription of the viral RNA (vRNA). Two viral surface glycoproteins (hemagglutinin and neuraminidase [NA]) are critical for virus binding and release and are the major viral antigens. The NS1 protein is a multifunctional factor that counteracts the cellular interferon (IFN) responses that are triggered upon influenza virus infection (4, 9, 12, 21, 29, 30, 48, 49). Other viral proteins play a critical role(s) in the nuclear export of newly synthesized viral replication complexes (i.e., the matrix protein M1 and the nuclear export protein NS2), virus entry (i.e., the ion channel protein M2), and the regulation of apoptosis (i.e., the PB1-F2 protein, which is not

encoded by all influenza A virus strains); the functions of these proteins are described in detail in reference 36.

Stimuli such as stress, cytokines, mitogens, and viral infections trigger multiple signaling cascades, such as the mitogen-activated protein kinase (MAPK) pathways, in mammalian cells (reviewed in references 10, 40, and 41). MAPK signaling pathways regulate critical cellular activities, such as gene expression, metabolism, apoptosis, mitosis, and differentiation. In the "classical" MAPK pathway, Raf-1 (a serine/threonine kinase) activates MEK1/2 (a MAPK kinase kinase), which subsequently activates the MAPK kinase extracellular signal-regulated kinases 1 and 2 (ERK1/2). In addition to ERK1/2, several other MAPK family members have been identified in mammalian cells, including p38 isoforms, c-Jun amino-terminal kinases, and BMK/ERK5 (big MAPK). MAPKs can activate their targets through direct phosphorylation or through the phosphorylation of downstream kinases (MAPK-activated protein kinases). Prominent examples of MAPK-activated protein kinases are p90 ribosomal S6 kinases (RSKs), which have emerged as major downstream mediators of ERK signal transduction (reviewed in references 6 and 41). In mammals, four RSKs (RSK1 to -4) have been identified; these are ubiquitously expressed and promote cell growth, proliferation, and cell survival (the last by interfering with apoptotic effectors). Despite their role as downstream mediators of ERK signal transduction, RSKs were not previously known to have antiviral effects.

Influenza virus infection has been shown to activate all known MAPK pathways (reviewed in references 26 and 27). Influenza virus-induced activation of the p38 and c-Jun amino-terminal kinase pathways seems to trigger antiviral effects (23,

* Corresponding author. Mailing address: Division of Virology, Department of Microbiology and Immunology, Institute of Medical Science, University of Tokyo, 4-6-1 Shirokanedai, Minato-ku, Tokyo 108-8639, Japan. Phone: 81-3-5449-5310. Fax: 81-3-5449-5408. E-mail: kawaoka@ims.u-tokyo.ac.jp.

25), while activation of the ERK1/2 and big MAPK pathways likely supports influenza virus replication (39). Further studies are needed to establish the significance of these signaling pathways for influenza virus replication.

Influenza virus infection also activates the IκB kinase/NF-κB pathway (reviewed in reference 19). This pathway is activated by a number of other viruses and leads to the expression of proinflammatory and antiviral cytokines, including beta IFN (IFN-β) and tumor necrosis factor alpha. The role of NF-κB activation in the context of influenza virus infection is still unclear, as two studies found a virus-supportive role (32, 50) and another study suggested that NF-κB activation is not required for efficient influenza virus replication (5).

In this study, we provide evidence that the MAPK-activated protein kinase ribosomal protein S6 kinase alpha 3 (RSK2) is activated upon influenza virus infection and that this kinase affects antiviral responses through NF-κB, IFN-β, and a known antiviral factor, PKR. These findings establish a novel antiviral role for RSK2.

## MATERIALS AND METHODS

**Cell culture.** Human embryonic kidney cells (293T cells and 293 cells) were cultured in Dulbecco's modified Eagle's medium (DMEM; Sigma) supplemented with 10% heat-inactivated fetal calf serum (FCS) and antibiotics. Plat-GP (murine leukemia virus-based packaging) cells were kindly provided by T. Kitamura (University of Tokyo, Tokyo, Japan) and cultured in DMEM with 10% FCS and 10 μg/ml blasticidin (Invitrogen). QT6 quail fibrosarcoma cells were maintained in Ham's F-12K medium (MP Biomedicals) supplemented with 10% FCS and 10% tryptose phosphate broth (Sigma). Madin-Darby canine kidney (MDCK) cells were cultured in minimal essential medium containing 5% newborn calf serum and antibiotics.

**Viruses.** PB2-627K- and PB2-627E-expressing influenza viruses were generated by reverse genetics (31) and propagated in MDCK cells. Both viruses possess the hemagglutinin and NA genes of A/WSN/33 (H1N1) virus, while the remaining genes were derived from A/Hong Kong/483/97 (H5N1) virus; the PB2 protein of this virus possesses a lysine at position 627, resulting in PB2K virus. PB2E virus is a derivative that possesses glutamic acid at position 627 in the PB2 protein. Influenza virus B/Hong Kong/73 and Sendai virus (Enders strain; kindly provided by Allan Portner, St. Jude Children's Research Hospital, Memphis, TN) were also propagated in MDCK cells. Viruses were titrated by plaque assay in MDCK cells.

**Plasmids.** The PB1, PA, and NP proteins of A/Hong Kong/483/97 (H5N1) virus were expressed with the pMX vector (34), which was kindly provided by T. Kitamura, University of Tokyo, Tokyo, Japan. For the PB2 protein, we used a variant that possesses glutamic acid at position 627 (PB2E). pPoII-fCD2 and pPoII-Luc drive the synthesis of negative-sense vRNAs comprising the 3' noncoding region of the NA (A/Hong Kong/483/97) vRNA, the complementary coding sequence of luciferase or feline CD2 (fCD2) (45), respectively, and the 5' noncoding region of the NA vRNA.

*Gallus gallus* RSK2 and human PKR were cloned from chicken embryo fibroblasts or human 293T cells, as appropriate. Briefly, RNA was extracted from these cells by use of the RNeasy minikit (Qiagen). Reverse transcription-PCR was performed with an oligo(dT) primer followed by PCR with gene-specific primers. The PCR products were cloned into the pCAGGS vector (under the control of the chicken β-actin promoter [33]) and then sequenced. To escape the knockdown effect of the short hairpin RNA (shRNA), a silent mutation was introduced into the human RSK2 protein expression plasmid, yielding pmRSK2.

pNF-κB-Luc, which expresses luciferase upon promoter activation by NF-κB, was purchased from Stratagene. pIFN-luc, which express luciferase under the control of an IFN-β-dependent promoter, was derived from the following components: the bacterial artificial chromosome clone RP11-113D19, which was used as the source of the promoter and terminator regions of the human IFN-β gene (Invitrogen), and pGEM-luc (Promega), which was used as the source of the luciferase gene. These components were joined by PCR, and the resulting construct was cloned into the pUC19 vector.

**cDNA library.** A cDNA library was prepared from quail QT6 cells by isolating mRNA (with the FastTrack 2.0 mRNA isolation kit; Invitrogen). cDNA was synthesized by use of the SuperScript Choice system for cDNA synthesis (In-

vitrogen), according to the manufacturer's instructions. The resulting cDNAs were size fractionated by agarose gel electrophoresis, and cDNA fragments longer than 1 kbp were extracted from the gel with the Qiaex II gel extraction kit (Qiagen). The respective cDNA fragments were then inserted into the BstXI sites of pCAGGS-Kan (a pCAGGS variant that carries the kanamycin resistance gene) by using BstXI adapters (Invitrogen). The ligated DNA was ethanol precipitated and then electroporated into DH10B competent cells.

**Library screening.** Human embryonic kidney 293T cells were transfected with plasmids for the expression of the polymerase and NP proteins, i.e., pMX-PB2E (possessing glutamic acid at position 627), -PB1, -PA, -NP; with the plasmid for the synthesis of a virus-like RNA encoding fCD2 (poII-fCD2); and with the quail QT6 cDNA library. Cells were incubated for 2 days at 33°C, collected, and treated with an antibody against fCD2 (44, 45). After incubation at 4°C for 30 min, fCD2-positive cells were selected by immunoaffinity with Bio-Adembeads goat anti-mouse immunoglobulin M (IgM) antibody (Ademtech) according to the manufacturer's instructions. Plasmid DNA was then extracted from the cells and amplified in *Escherichia coli* in Luria-Bertani medium supplemented with kanamycin. Selection of cells that expressed high levels of fCD2 was repeated four times, at which point plasmid DNA was extracted from the cells and sequenced.

**Luciferase assay.** Luciferase assays were performed by use of a dual-luciferase reporter assay system (Promega) on a microplate luminometer (Veritas; Turner Biosystems, Sunnyvale, CA), according to the manufacturer's instructions. As an internal control for the dual-luciferase assay, pGL4.74[hRluc/TK] (Promega) was used.

**Construction of RSK2 knockdown cells by use of a retroviral vector.** shRNA with a human RSK2 target sequence (5'-GATGCTGCTTGTGATATATGG-3') was flanked by the mU6 promoter and terminator. The resulting cDNA was inserted into the pSSSP vector, which was kindly provided by H. Iba (University of Tokyo, Tokyo, Japan). A similar plasmid, pSSSP-shGFP, with a target sequence for green fluorescent protein (GFP) (5'-GCCACAACGTCTATATCA TGG-3') was also kindly provided by H. Iba (University of Tokyo, Tokyo, Japan). These plasmids were used to produce murine leukemia virus-based viruses in Plat-GP cells, as described previously (20, 45), and then used to transduce 293 cells.

**Analysis of virus propagation.** To establish virus growth rates, three wells of cells were infected in parallel with virus at a multiplicity of infection (MOI) of 0.05 and incubated at 33°C or 37°C. At various times, supernatants were assayed to determine the titer of the infectious virus by plaque assay of MDCK cells.

**NF-κB and IFN-β promoter activity.** pNF-κB-Luc and pIFN-luc were transfected into 293 (human embryonic kidney) cells with a retroviral vector expressing shRNA specific to human RSK2 (shRSK2 cells) and shGFP cells, respectively. Nine hours later, cells were infected with virus at an MOI of 1.0 and incubated at 33°C. Twelve hours later, the levels of luciferase expression were determined.

**Western blot analysis.** To assess RSK2 expression levels, shRSK2 cells and shGFP cells were suspended in Tris-glycine sodium dodecyl sulfate (SDS) sample buffer (Invitrogen), and Western blot analysis was performed with anti-RSK2 (E1; Santa Cruz Biotechnology) and anti-β-actin (as an internal control; Sigma) antibodies, according to the manufacturers' instructions. Biotinylated anti-mouse IgG antibody (Vector) was used as a secondary antibody. Bands were detected with the Vectastain ABC kit (Vector) and ECL Plus Western blotting detection reagents (GE Healthcare); the VersaDoc imaging system (Bio-Rad) was used to quantify band intensities.

To analyze expression of the viral M1 protein, shRSK2 cells and control shGFP cells were infected with a PB2-627E-expressing virus at an MOI of 1.0 and incubated at 33°C. At various times, the cells were washed three times with phosphate-buffered saline and resuspended in Tris-glycine SDS sample buffer. Western blot analysis was performed with monoclonal antibodies specific to the M1 protein, with β-actin as a control. Biotinylated anti-mouse IgG antibody (Vector) was used as a secondary antibody. Bands were detected as described above.

To assess RSK2 phosphorylation levels, 293 cells ($7.5 \times 10^5$ cells) were plated in 60-mm plates and cultured overnight at 37°C. The growth medium was replaced with DMEM containing 4% bovine serum albumin, and cells were infected with influenza virus (MOI of 3.0) 12 hours later; control cells remained uninfected. Three hours postinfection, RSK2 was immunoprecipitated with anti-RSK2 antibody (E1; Santa Cruz) coupled to protein G beads. The beads were resuspended in Tris-glycine SDS sample buffer, and Western blot analysis was performed with antibodies specific for RSK phosphorylated at Thr365/Ser369, Ser386, or Thr577 (antibodies obtained from Cell Signaling). Biotinylated anti-rabbit IgG antibody (Vector) was used as a secondary antibody. Bands were detected as described above.
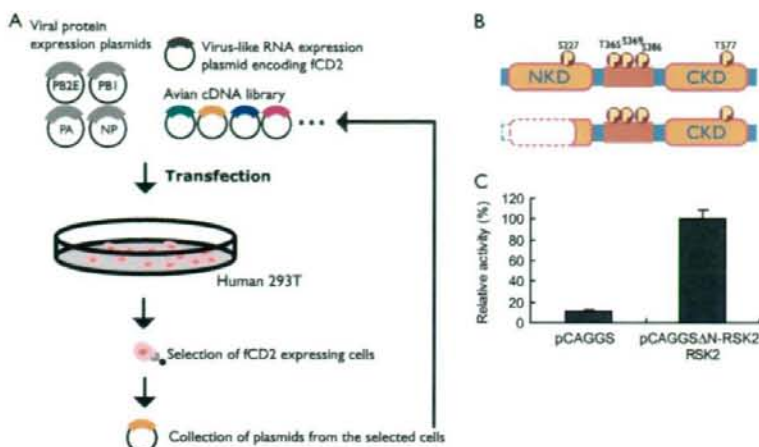
FIG. 1. Identification of cellular proteins that enhance influenza virus replication and downregulation of influenza virus replication by RSK2. (A) Human embryonic kidney 293T cells were transfected with plasmids encoding the components of the influenza viral replication complex (PB2, PB1, PA, and NP). The PB2 protein possesses glutamic acid at position 627 (PB2-627E), which supports efficient replication in avian cells but not in mammalian cells at 33°C. Cells were cotransfected with a plasmid for the synthesis of a virus-like RNA encoding fCD2 (polI-fCD2) and with an avian (quail cell) cDNA library. Cells expressing avian proteins that support efficient replication by PB2-627E virus in mammalian cells at 33°C will produce increased amounts of fCD2. Cells with high levels of fCD2 were selected by immunoaffinity using anti-fCD2 antibody. After a total of four rounds of selection, plasmid DNA was extracted from the cells and sequenced. (B) Schematic diagram of human RSK2 (top) and the N-terminally deleted avian RSK2 protein selected in our screening approach (bottom). The CKD is activated by ERK1/2, resulting in the activation of the NKD. The NKD subsequently phosphorylates target proteins. (C) Influenza viral polymerase activity in 293T cells expressing avian ΔN-RSK2. Cells were transfected with plasmids expressing PB2E, PB1, PA, and NP; a virus-like RNA encoding luciferase (pPolI-luc); and the N-terminally deleted avian RSK2 protein (pCAGGS-ΔN-RSK2) or the "empty" control vector (pCAGGS). Cells were maintained at 33°C for 24 h and were then subjected to luciferase assays. In human cells at 33°C, expression of N-terminally deleted avian RSK2 increased the activity of a replication complex possessing glutamic acid at position 627 in the PB2 protein. The error bars represent standard deviations from three independent experiments.

To assess the phosphorylation levels of PKR, shRSK2 and control shGFP cells were infected at an MOI of 0.01 or 1.0 with influenza virus and incubated at 33°C. Infected cells were collected at 0, 6, and 12 h postinfection. Western blot analysis was performed with anti-PKR (Santa Cruz), anti-phospho-PKR (Biosource), and anti-β-actin (as an internal control; Sigma) antibodies according to the manufacturers' instructions. Biotinylated anti-rabbit IgG antibody or anti-mouse IgG antibody was used as a secondary antibody. Bands were detected as described above.

**Statistical analysis.** Student's *t* test was used to determine statistical significance.

## RESULTS AND DISCUSSION

Relatively little is known about the host factors that interact with influenza virus components. The influenza virus PB2 protein is now recognized as a critical determinant of pathogenicity and host range restriction (16, 17, 28, 46, 47). In general, lysine 627 of the PB2 protein confers a high level of pathogenicity to influenza viruses in mammals (16), which can be modeled by efficient replication in mammalian cells at 33°C and 37°C (17). In contrast, viruses with a glutamic acid residue at this position (PB2-627E) have low pathogenicity in mammals (16) and attenuated virus replication in mammalian systems at 33°C and, to a lesser extent, at 37°C (17). In order to identify the host factor(s) that restricts PB2-627E virus growth in mammalian cells, we transfected human embryonic kidney (293T) cells with a plasmid for synthesis of an influenza virus-like RNA. This virus-like RNA encodes fCD2; fCD2 thus serves as a reporter protein (45) to assess viral replication efficiencies. We cotransfected cells with plasmids for expres-

sion of the A/Hong Kong/483/97 (H5N1) virus NP, PB1, and PA proteins and a plasmid for expression of a mutant PB2, PB2-627E (Fig. 1A). The PB2-627E mutation restricts amplification of the virus-like RNA in human cells at 33°C. To identify the avian host factor(s) that "rescues" efficient replication, even with PB2-627E, we cotransfected human 293T cells with a cDNA expression library derived from avian quail QT6 cells. Avian host factors that mediate efficient replication of PB2-627E virus should support high levels of fCD2 expression from the virus-like RNA. The fCD2-positive cells were selected with an antibody against fCD2. After four rounds of selection, we extracted plasmids from the fCD2-positive transfectants and subjected them to sequencing.

One of the identified host proteins was the quail homolog of the *Gallus gallus* RSK2, from which 310 N-terminal amino acids were missing (avian ΔN-RSK2) (Fig. 1B). To confirm that avian ΔN-RSK2 enhances influenza virus replication in mammalian cells at 33°C, we overexpressed this protein in human cells that expressed the viral replication complex components (i.e., PB2-627E, PB1, PA, and NP) and a virus-like RNA that encodes the luciferase reporter protein. Our results indicate that luciferase expression was elevated in cells expressing avian ΔN-RSK2 protein relative to that in control cells expressing the "empty" expression vector (Fig. 1C).

Next, we cloned the full-length avian and human RSK2 proteins and tested their ability to enhance PB2-627E-mediated replication in human cells at 33°C; however, we did not detect a significant effect for either protein (data not shown).
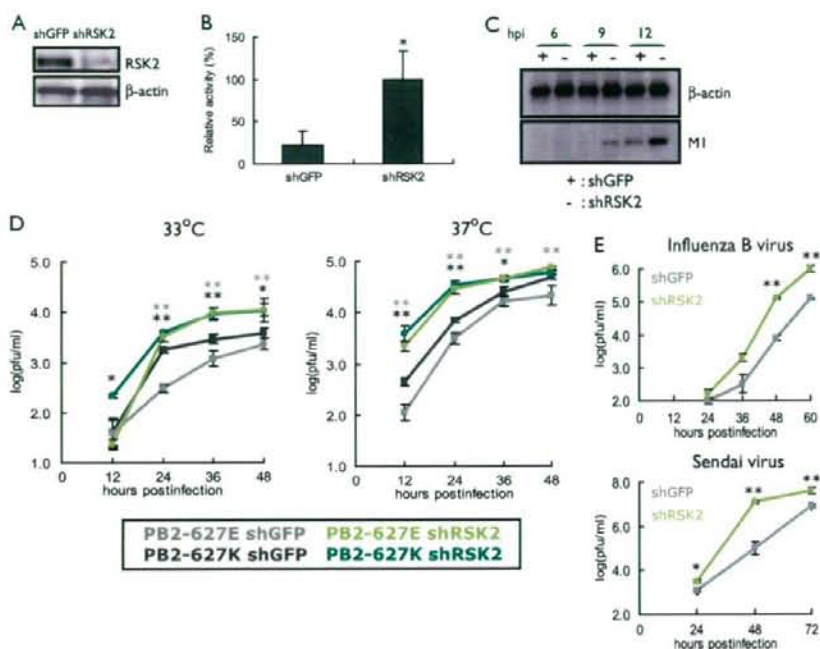
FIG. 2. Effect of RSK2 knockdown on influenza virus replication. (A) Knockdown of human RSK2. 293 cells were transduced with retroviral vectors for shRNAs to human RSK2 or GFP (as a control), resulting in shRSK2 and shGFP cells. RSK2 expression levels were assessed by Western blotting with an antibody to this protein. β-Actin expression levels served as an internal control. (B) Viral polymerase activity in shRSK2 and shGFP cells. Cells were transfected with plasmids that directed synthesis of PB2-627E, PB1, PA, NP, and pPolI-luc. After incubation at 33°C for 24 h, cell lysates were prepared and subjected to luciferase assays. Knockdown of RSK2 resulted in more-efficient replication of the virus-like RNA, suggesting that RSK2 suppresses influenza virus replication. The error bars represent standard deviations from three independent experiments. The statistical significance of the difference between the control and test samples is shown by the $P$ value, which was determined by Student's $t$ test (*, $P < 0.05$). (C) Viral protein production in shRSK2 cells and shGFP cells. shRSK2 and shGFP cells were infected with virus possessing PB2-627E and incubated at 33°C. At the indicated time points postinfection, Western blot analysis was carried out with antibodies against M1 and β-actin. (D) Influenza A virus growth in shRSK2 cells. shRSK2 and control shGFP cells were infected at an MOI of 0.05 with PB2-627E or PB2-627K virus, which possesses glutamic acid or lysine at position 627 in the PB2 protein, respectively. Cells were incubated at 33°C or 37°C for the indicated time periods. Virus titers in MDCK cells were determined. The error bars represent standard deviations from three independent experiments. The statistical significance of the difference between the control and test samples is shown by $P$ values, which were determined by Student's $t$ test (**, $P < 0.01$; *, $P < 0.05$; black asterisks indicate the PB2-627K virus, and gray asterisks indicate the PB2-627E virus). (E) Influenza B virus and Sendai virus growth in shRSK2 cells. shRSK2 and control shGFP cells were infected at an MOI of 0.05 with influenza B virus or Sendai virus. At the indicated times after infection, cells were harvested and the virus titers in MDCK cells were determined. The error bars represent standard deviations from three independent experiments. The statistical significance of the difference between the control and test samples is shown by the $P$ value, which was determined by Student's $t$ test (**, $P < 0.01$; *, $P < 0.05$).

RSK family members are unusual among serine/threonine kinases in that they contain two distinct kinase domains that are sequentially activated (Fig. 1B). The C-terminal kinase domain (CKD) is activated by ERK1/2, which then triggers subsequent activation of the N-terminal kinase domain (NKD) (reviewed in reference 6). The NKD of RSK2 then phosphorylates a broad range of substrates, including cAMP response element-binding protein, c-Fos, glycogen synthase kinase 3, and many others (reviewed in reference 6). ΔN-RSK2 contains the entire CKD of this protein (Fig. 1B) and may sequester free ERK1/2, thereby preventing activation of functional RSK2. Thus, we speculated that full-length RSK2 has antiviral activity and that ΔN-RSK2 acts as a dominant-negative factor that suppresses RSK2 and its antiviral activity, resulting in increased viral replication.

To test our hypothesis that RSK2 has antiviral activity

against influenza virus, we knocked down RSK2 in 293 (human embryonic kidney) cells using a retroviral vector expressing shRNA specific to human RSK2. RSK2 expression was reduced to approximately 15% in shRSK2 cells relative to the expression level in control shGFP cells, which express shRNA against GFP (Fig. 2A). As speculated, RSK2 knockdown resulted in increased viral polymerase activity for PB2-627E at 33°C (Fig. 2B) and, as a consequence, resulted in increased production of the viral M1 protein (Fig. 2C).

The data obtained thus far indicate that RSK2 suppresses influenza virus replication. However, the question of whether RSK2 interferes with influenza virus replication in general or in a strain- or host-specific manner remains unanswered. To address this question, we generated influenza viruses that possessed either a lysine at position 627 of PB2 (PB2-627K), which confers efficient replication in mammalian cells at 33°C and
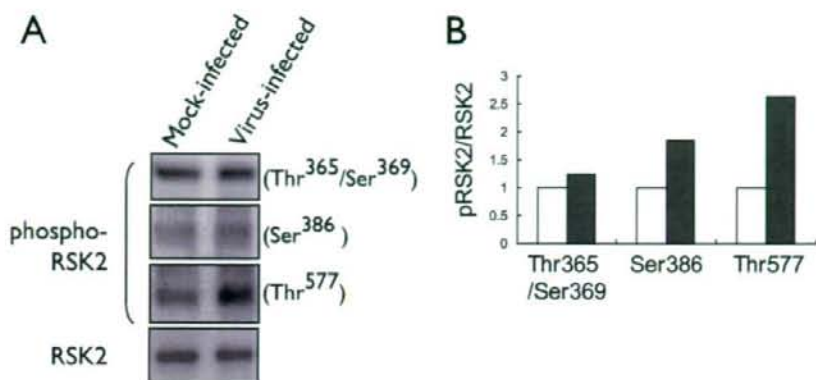
FIG. 3. Influenza virus-induced phosphorylation of RSK2. (A) 293 cells were infected with the PB2-627K virus (MOI of 3.0) or remained mock infected. Three or 5 hours later, cell lysates were immunoprecipitated with anti-RSK2 antibody, followed by Western blot analysis with the indicated antibodies to phosphorylated forms of RSK2. (B) Graphical representation of data shown in panel A. The relative ratios of phosphorylated to nonphosphorylated RSK2 are depicted. Influenza virus infection results in phosphorylation of RSK2. White bars, mock-infected cells; black bars, virus-infected cells.

37°C, or a glutamic acid at this position (PB2-627E), which results in attenuation of replication in mammalian cells at 33°C and, to a lesser extent, at 37°C. Growth of both viruses at 33°C and 37°C in shRSK2 cells and control shGFP cells was tested. Briefly, cells were infected at an MOI of 0.05 with PB2-627E or PB2-627K virus and virus titers in the culture supernatant were determined by plaque formation assays of MDCK cells at various times postinfection. As expected, the PB2-627K virus grew more efficiently than the PB2-627E virus in control shGFP cells at 33°C (Fig. 2D, left), while only minor differences in growth were observed for PB2-627K and PB2-627E viruses in control shGFP cells at 37°C (Fig. 2D, right); these findings are consistent with our earlier data (17). By comparing viral growth properties in control shGFP and shRSK2 cells, we found more-efficient growth in shRSK2 cells for both viruses at both temperatures, demonstrating that the nature of the amino acid at position 627 of PB2 does not affect the antiviral effect mediated by RSK2; all subsequent infection experiments were therefore carried out with the PB2-627K virus. Together, these findings indicate that RSK2 is a general antiviral host factor that suppresses influenza A virus replication.

To further examine the antiviral function of RSK2, we assessed the growth kinetics of an influenza B virus and Sendai virus (a negative-sense RNA virus belonging to the family *Paramyxoviridae*) in shRSK2 and shGFP control cells (Fig. 2E). These viruses grew more efficiently in shRSK2 cells than in control shGFP cells. Hence, RSK2 may have broad antiviral effects; for example, it may trigger an innate immune responses.

In quiescent cells, RSK2 is maintained in an inactive form in a complex with ERK1/2 (reviewed in reference 42). Interaction with phosphorylated ERK1/2 results in RSK2 phosphorylation, dissociation from ERK1/2, and (partial) translocation to the nucleus (7). To assess whether RSK2 is activated upon influenza virus infection, we immunoprecipitated RSK2 from cell lysates obtained from influenza virus- or mock-infected cells and subsequently evaluated the phosphorylation status of RSK2 using antibodies specific to distinct phosphorylated

forms of RSK2. Influenza virus infection resulted in increased levels of phosphorylated RSK2 compared to those in mock-infected cells (Fig. 3A and B). The most efficient induction of phosphorylation was observed for Thr577. This residue is phosphorylated by ERK1/2, resulting in the activation of RSK2 and the subsequent autophosphorylation of other phosphorylation sites, such as Ser386 (reviewed in reference 6). The observed phosphorylation of RSK2 upon influenza infection may result from direct interaction with a viral component or from ERK1/2 signaling, as the "classical" MAPK (Raf/MEK/ERK) pathway is known to be activated by influenza virus infection (38).

Next, we assessed the mechanism(s) by which RSK2 affects influenza virus replication. RSK2 activates NF-κB (13, 43), a major player in innate immune responses to viral infections (reviewed in reference 19). Moreover, NF-κB is known to be activated upon influenza virus infection (35). Therefore, we speculated that influenza virus-induced activation of RSK2 may lead to the stimulation of NF-κB and subsequent induction of an antiviral response. To test this assumption, we expressed the luciferase reporter protein under the control of an NF-κB-dependent promoter in virus- or mock-infected shRSK2 and control shGFP cells (Fig. 2A). As expected, influenza A virus infection induced NF-κB promoter activity in shGFP cells (Fig. 4A); the level of promoter stimulation was similar to that published elsewhere (52). In contrast, no significant increase in NF-κB-dependent promoter activity was observed in virus-infected shRSK2 cells (Fig. 4A), suggesting that virus-induced NF-κB stimulation relies on RSK2 activation. This lack of activation was partially restored following transfection of shRSK2 cells with pmRSK2, which encodes a human RSK2 cDNA containing a silent mutation within the small interfering RNA target sequence (Fig. 4A). In conclusion, these findings suggest that RSK2 may affect influenza virus replication, at least in part, through NF-κB.

NF-κB stimulation leads to the expression of multiple cellular factors, including IFN-β, a central player in the innate immune response that is activated upon virus infection. We asked whether RSK2 activates IFN-β-stimulated promoters.
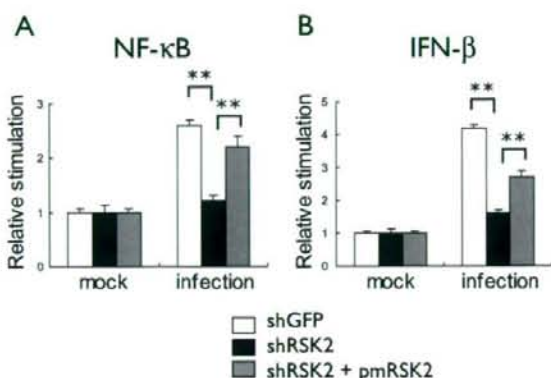
FIG. 4. Effect of RSK2 knockdown on influenza virus-induced activation of NF-κB- and IFN-β-dependent promoters. Plasmids that express luciferase under the control of NF-κB (A)- or IFN-β-dependent (B) promoters were transfected into shRSK2 or control shGFP cells. Nine hours posttransfection, cells were infected with the PB2-627K virus at an MOI of 1; control cells remained mock infected. After 12 hours of incubation at 33°C, cell lysates were prepared and subjected to luciferase assays. In a parallel experiment, cells were also transfected with pmRSK2, which encodes a silently mutagenized human RSK2 that is not recognized by the RSK2 shRNA. Influenza virus induced stimulation of NF-κB- and IFN-β-dependent promoters in shGFP cells (white bars); this stimulation is blocked by RSK2 knockdown (black bars) but can be partially restored upon expression of RSK2 that is insensitive to the RSK2 shRNA (gray bars). The error bars represent standard deviations from three independent experiments. $P$ values were determined by Student's $t$ test (∗∗, $P < 0.01$).

We carried out experiments essentially as described in the previous section. That is, we cloned the luciferase gene under the control of an IFN-β-stimulated promoter and assayed luciferase expression in virus- and mock-infected shRSK2 and control shGFP cells (Fig. 4B). Influenza virus infection activated IFN-β-stimulated promoter activity in control shGFP cells (Fig. 4B) but not in shRSK2 cells (Fig. 4B). This impediment was partially overcome by transfection of shRSK2 cells with pmRSK2 (Fig. 4B). These results demonstrate that RSK2 activates both NF-κB and IFN-β signaling pathways upon influenza infection in 293 cells.

PKR is an important component of IFN-mediated antiviral responses (reviewed in reference 15). This kinase phosphorylates the α subunit of eukaryotic initiation factor 2, resulting in rapid inhibition of translation and restriction of the spread of the virus (2, 3, 11, 14). Recently, PKR was also identified as an RSK2 substrate (53). We tested whether RSK2 affects influenza virus replication through PKR phosphorylation and activation. As expected, phosphorylation of PKR upon influenza virus infection was apparent in control shGFP cells (Fig. 5A; Fig. 5B shows an increasing ratio of phosphorylated to nonphosphorylated PKR upon virus infection). In contrast, PKR phosphorylation was suppressed in shRSK2 cells (Fig. 5A and B), indicating that influenza virus-induced activation of RSK2 results in PKR phosphorylation in 293 cells.

In summary, we demonstrated that the MAPK-activated protein kinase RSK2 plays a role in the innate immune response to influenza virus infection, as shown in Fig. 6. RSK2 is known to phosphorylate cellular factors involved in cell prolif-
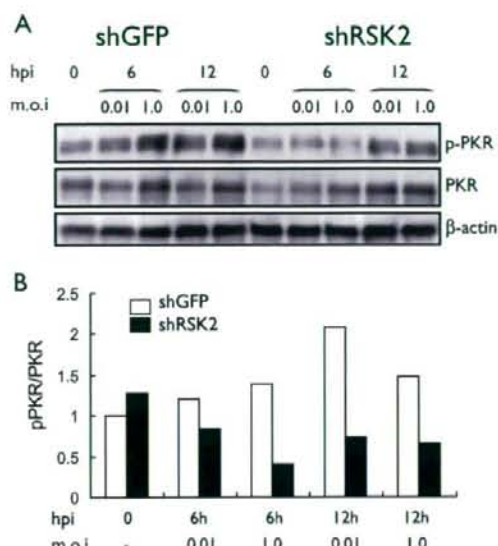


FIG. 5. Effect of RSK2 knockdown on influenza virus-induced phosphorylation of PKR. (A) shRSK2 cells and control shGFP cells were infected with the PB2-627K virus at an MOI of 0.01 or 1 and incubated at 33°C. At the indicated times postinfection, cell lysates were prepared and subjected to Western blot analysis with antibodies against PKR, phosphorylated PKR, or β-actin, which served as an internal control. hpi, hours postinfection. (B) Graphical representation of data shown in panel A. The relative ratios of phosphorylated to nonphosphorylated PKR are depicted. Influenza virus infection results in increased levels of phosphorylated PKR in control shGFP cells but not in shRSK2 cells.

eration, regulation of transcription, regulation of translation, cell survival, and apoptosis (reviewed in reference 6) and may affect viral growth through these processes. The human immunodeficiency virus Tat protein is known to interact with RSK2 (18), resulting in RSK2 activation. Activated RSK2 is, in turn,
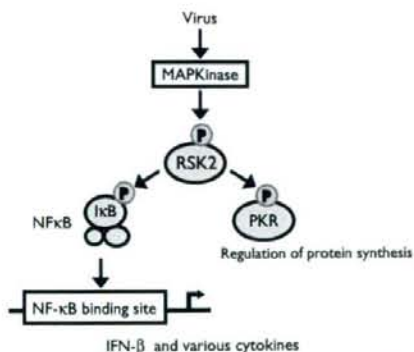


FIG. 6. Putative role of RSK2 in antiviral signaling. Influenza virus infection may activate RSK2 through MAPK kinase signaling pathways or through direct interaction with a viral component. Our data suggest that RSK2 activation is needed for efficient stimulation of NF-κB, IFN-β, and PKR, all of which play major roles in the cellular antiviral response.

critical for the transcriptional activity of Tat (18). Another study demonstrated that ORF45 of the Kaposi's sarcoma-associated herpesvirus interacts with RSK1 and RSK2, resulting in their stimulation (22). Further studies suggest that RSK1/2 upregulation plays a critical role in the lytic replication of Kaposi's sarcoma-associated herpesvirus (22). Another study suggested that RSK2 signaling is important for efficient vaccinia virus amplification (1). It is interesting to note that these studies ascribe a virus-supportive role to RSK2 activation.

In contrast to the above-mentioned studies, which found a virus-supportive role for RSK2, our findings suggest an antiviral activity for this kinase. In particular, we found that the C-terminal domain of RSK2, which acts in a dominant-negative manner, and a small interfering RNA to RSK2 increased influenza virus polymerase activity in in vitro assays and/or enhanced influenza virus replication. RSK2 is known to be activated by the Raf/MEK/ERK signaling cascade (reviewed in reference 24). Studies by Pleschka et al. (39) suggest that this pathway has a virus-supportive function. This finding seems to contradict our finding that RSK2 has antiviral activity. However, the virus-supportive function of the Raf/MEK/ERK signaling cascade was established by use of an inhibitor to MEK (39), which may affect several pathways that are controlled by MEK/ERK. In addition, activation of RSK1/2 is controlled not only by ERK1/2, but also by other MAPKs, such as p38 (reviewed in references 10 and 40), which is activated upon influenza virus infection and triggers an antiviral response (8). Collectively, the current data suggest that RSK2 is activated by both virus-supportive and -antagonistic signaling pathways and that the complex interplay of these factors and pathways determines its downstream effects.

Our data suggest that RSK2 may execute its antiviral function through NF-κB. Some studies have found a supportive role for NF-κB in influenza virus infection (32, 50), while another study suggested that NF-κB activation is not required for efficient influenza virus replication (5). In general, the role of NF-κB in the regulation of IFN-β responses is still not well understood. Recent studies found that NF-κB stimulates the expression of certain IFN-stimulated genes, while it suppresses others (37). As discussed earlier, viral infections trigger multiple cellular pathways that stimulate both agonistic and antagonistic functions; the outcome of a viral infection may ultimately be determined by the complex and as yet poorly understood interplay between these virus-supportive and -antagonistic factors.

We found that RSK2 affects influenza virus replication through innate immune response pathways (Fig. 6). Although RSK2 is known to activate NF-κB (13, 43) and PKR (53), it had not been recognized as a critical signaling component in innate immune responses to viral infections. We found, however, that RSK2 knockdown in 293 cells affected the influenza virus-induced activation of NF-κB and IFN-β and the influenza virus-induced phosphorylation of PKR, suggesting a critical role for RSK2 in innate immune responses to viral infections. In fact, we found that RSK2 knockdown not only increased influenza A virus titers but also stimulated influenza B virus and Sendai virus replication. In conclusion, we have identified a role for RSK2 in innate immune responses to influenza A virus infection, which may be executed through the regulation of IFN-β, NF-κB, and PKR responses. Other

MAPK-activated protein kinases may have similar, as of yet unidentified, functions in the innate immune response and antiviral defense mechanisms.

## REFERENCES

1. **Andrade, A. A., P. N. Silva, A. C. Pereira, L. P. De Sousa, P. C. Ferreira, R. T. Gazzinelli, E. G. Kroon, C. Ropert, and C. A. Bonjardim.** 2004. The vaccinia virus-stimulated mitogen-activated protein kinase (MAPK) pathway is required for virus multiplication. Biochem. J. **381:**437–446.
2. **Balachandran, S., P. C. Roberts, L. E. Brown, H. Truong, A. K. Pattnaik, D. R. Archer, and G. N. Barber.** 2000. Essential role for the dsRNA-dependent protein kinase PKR in innate immunity to viral infection. Immunity **13:**129–141.
3. **Barber, G. N.** 2005. The dsRNA-dependent protein kinase, PKR and cell death. Cell Death Differ. **12:**563–570.
4. **Bergmann, M., A. Garcia-Sastre, E. Carnero, H. Pehamberger, K. Wolff, P. Palese, and T. Muster.** 2000. Influenza virus NS1 protein counteracts PKR-mediated inhibition of replication. J. Virol. **74:**6203–6206.
5. **Bernasconi, D., C. Amici, S. La Frazia, A. Ianaro, and M. G. Santoro.** 2005. The IkappaB kinase is a key factor in triggering influenza A virus-induced inflammatory cytokine production in airway epithelial cells. J. Biol. Chem. **280:**24127–24134.
6. **Carriere, A., H. Ray, J. Blenis, and P. P. Roux.** 2008. The RSK factors of activating the Ras/MAPK signaling cascade. Front. Biosci. **13:**4258–4275.
7. **Chen, R. H., C. Sarnecki, and J. Blenis.** 1992. Nuclear localization and regulation of *erk*- and *rsk*-encoded protein kinases. Mol. Cell. Biol. **12:**915–927.
8. **Conze, D., J. Lumsden, H. Enslen, R. J. Davis, G. Le Gros, and M. Rincón.** 2000. Activation of p38 MAP kinase in T cells facilitates the immune response to the influenza virus. Mol. Immunol. **37:**503–513.
9. **Donelan, N. R., C. F. Basler, and A. García-Sastre.** 2003. A recombinant influenza A virus expressing an RNA-binding-defective NS1 protein induces high levels of beta interferon and is attenuated in mice. J. Virol. **77:**13257–13266.
10. **Gaestel, M.** 2008. Specificity of signaling from MAPKs to MAPKAPKs: kinases' tango nuevo. Front. Biosci. **13:**6050–6059.
11. **Gale, M., Jr., and M. G. Katze.** 1998. Molecular mechanisms of interferon resistance mediated by viral-directed inhibition of PKR, the interferon-induced protein kinase. Pharmacol. Ther. **78:**29–46.
12. **Geiss, G. K., M. Salvatore, T. M. Tumpey, V. S. Carter, X. Wang, C. F. Basler, J. K. Taubenberger, R. E. Bumgarner, P. Palese, M. G. Katze, and A. García-Sastre.** 2002. Cellular transcriptional profiling in influenza A virus-infected lung epithelial cells: the role of the nonstructural NS1 protein in the evasion of the host innate defense and its potential contribution to pandemic influenza. Proc. Natl. Acad. Sci. USA **99:**10736–10741.
13. **Ghoda, L., X. Lin, and W. C. Greene.** 1997. The 90-kDa ribosomal S6 kinase (pp90rsk) phosphorylates the N-terminal regulatory domain of IkappaBalpha and stimulates its degradation in vitro. J. Biol. Chem. **272:**21281–21288.
14. **Goodman, A. G., J. A. Smith, S. Balachandran, O. Perwitasari, S. C. Proll, M. J. Thomas, M. J. Korth, G. N. Barber, L. A. Schiff, and M. G. Katze.** 2007. The cellular protein P58IPK regulates influenza virus mRNA translation and replication through a PKR-mediated mechanism. J. Virol. **81:**2221–2223.
15. **Haller, O., G. Kochs, and F. Weber.** 2007. Interferon, Mx, and viral countermeasures. Cytokine Growth Factor Rev. **18:**425–433.
16. **Hatta, M., P. Gao, P. Halfmann, and Y. Kawaoka.** 2001. Molecular basis for high virulence of Hong Kong H5N1 influenza A viruses. Science **293:**1840–1842.
17. **Hatta, M., Y. Hatta, J. H. Kim, S. Watanabe, K. Shinya, T. Nguyen, P. S. Lien, Q. M. Le, and Y. Kawaoka.** 2007. Growth of H5N1 influenza A viruses in the upper respiratory tracts of mice. PLoS Pathog. **3:**1374–1379.
18. **Hetzer, C., D. Bisgrove, M. S. Cohen, A. Pedal, K. Kaehlcke, A. Speyerer, K. Bartscherer, J. Taunton, and M. Ott.** 2007. Recruitment and activation of RSK2 by HIV-1 Tat. PLoS ONE **2:**e151.
19. **Hiscott, J., H. Kwon, and P. Génin.** 2001. Hostile takeovers: viral appropriation of the NF-kappaB pathway. J. Clin. Investig. **107:**143–151.
20. **Kitamura, T., and Y. Morikawa.** 2000. Isolation of T-cell antigens by retrovirus-mediated expression cloning. Methods Mol. Biol. **134:**143–152.
21. **Kochs, G., A. García-Sastre, and L. Martínez-Sobrido.** 2007. Multiple anti-

interferon actions of the influenza A virus NS1 protein. J. Virol. 81:7011–7021.
22. Kuang, E., Q. Tang, G. G. Maul, and F. Zhu. 2008. Activation of p90 ribosomal S6 kinase by ORF45 of Kaposi's sarcoma-associated herpesvirus and its role in viral lytic replication J. Virol. 82:1838–1850.
23. Kujime, K., S. Hashimoto, Y. Gon, K. Shimizu, and T. Horie. 2000. p38 mitogen-activated protein kinase and c-jun-NH2-terminal kinase regulate RANTES production by influenza virus-infected human bronchial epithelial cells. J. Immunol. 164:3222–3228.
24. Lu, Z., and S. Xu. 2006. ERK1/2 MAP kinases in cell survival and apoptosis. IUBMB Life 58:621–631.
25. Ludwig, S., C. Ehrhardt, E. R. Neumeier, M. Kracht, U. R. Rapp, and S. Pleschka. 2001. Influenza virus-induced AP-1-dependent gene expression requires activation of the JNK signaling pathway. J. Biol. Chem. 276:10990–10998.
26. Ludwig, S., O. Planz, S. Pleschka, and T. Wolff. 2003. Influenza-virus-induced signaling cascades: targets for antiviral therapy? Trends Mol. Med. 9:46–52.
27. Ludwig, S., S. Pleschka, O. Planz, and T. Wolff. 2006. Ringing the alarm bells: signalling and apoptosis in influenza virus infected cells. Cell. Microbiol. 8:375–386.
28. Massin, P., S. van der Werf, and N. Naffakh. 2001. Residue 627 of PB2 is a determinant of cold sensitivity in RNA replication of avian influenza viruses. J. Virol. 75:5398–5404.
29. Mibayashi, M., L. Martínez-Sobrido, Y. M. Loo, W. B. Cárdenas, M. Gale, Jr., and A. García-Sastre. 2007. Inhibition of retinoic acid-inducible gene I-mediated induction of beta interferon by the NS1 protein of influenza A virus. J. Virol. 81:514–524.
30. Min, J. Y., and R. M. Krug. 2006. The primary function of RNA binding by the influenza A virus NS1 protein in infected cells: inhibiting the 2'-5' oligo(A) synthetase/RNase L pathway. Proc. Natl. Acad. Sci. USA 103:7100–7105.
31. Neumann, G., T. Watanabe, H. Ito, S. Watanabe, H. Goto, P. Gao, M. Hughes, D. R. Perez, R. Donis, E. Hoffmann, G. Hobom, and Y. Kawaoka. 1999. Generation of influenza A viruses entirely from cloned cDNAs. Proc. Natl. Acad. Sci. USA 96:9345–9350.
32. Nimmerjahn, F., D. Dudziak, U. Dirmeier, G. Hobom, A. Riedel, M. Schlee, L. M. Staudt, A. Rosenwald, U. Behrends, G. W. Bornkamm, and J. Mautner. 2004. Active NF-kappaB signalling is a prerequisite for influenza virus infection. J. Gen. Virol. 85:2347–2356.
33. Niwa, H., K. Yamamura, and J. Miyazaki. 1991. Efficient selection for high-expression transfectants with a novel eukaryotic vector. Gene 108:193–199.
34. Onishi, M., S. Kinoshita, Y. Morikawa, A. Shibuya, J. Phillips, L. L. Lanier, D. M. Gorman, G. P. Nolan, A. Miyajima, and T. Kitamura. 1996. Applications of retrovirus-mediated expression cloning. Exp. Hematol. 24:324–329.
35. Pahl, H. L., and P. A. Baeuerle. 1995. Expression of influenza virus hemagglutinin activates transcription factor NF-κB. J. Virol. 69:1480–1484.
36. Palese, P. 2007. Orthomyxoviridae, p. 1649–1689. In D. M. Knipe, P. M. Howley, D. E. Griffin, R. A. Lamb, M. A. Martin, B. Roizman, and S. E. Straus (ed.), Fields virology, 5th ed. Lippincott Williams & Wilkins, Philadelphia, PA.
37. Pfeffer, L. M., J. G. Kim, S. R. Pfeffer, D. J. Carrigan, D. P. Baker, L. Wei, and R. Homayouni. 2004. Role of nuclear factor-kappaB in the antiviral action of interferon and interferon-regulated gene expression. J. Biol. Chem. 279:31304–31311.
38. Pleschka, S. 2008. RNA viruses and the mitogenic Raf/MEK/ERK signal transduction cascade. Biol. Chem. [Epub ahead of print] doi:10.1515/BC.2008.145.
39. Pleschka, S., T. Wolff, C. Ehrhardt, G. Hobom, O. Planz, U. R. Rapp, and S. Ludwig. 2001. Influenza virus propagation is impaired by inhibition of the Raf/MEK/ERK signalling cascade. Nat. Cell Biol. 3:301–305.
40. Raman, M., W. Chen, and M. H. Cobb. 2007. Differential regulation and properties of MAPKs. Oncogene 26:3100–3112.
41. Roux, P. P., and J. Blenis. 2004. ERK and p38 MAPK-activated protein kinases: a family of protein kinases with diverse biological functions. Microbiol. Mol. Biol. Rev. 68:320–344.
42. Roux, P. P., S. A. Richards, and J. Blenis. 2003. Phosphorylation of p90 ribosomal S6 kinase (RSK) regulates extracellular signal-regulated kinase docking and RSK activity. Mol. Cell. Biol. 23:4796–4804.
43. Schouten, G. J., A. C. Vertegaal, S. T. Whiteside, A. Israël, M. Toebes, J. C. Dorsman, A. J. van der Eb, and A. Zantema. 1997. IkappaB alpha is a target for the mitogen-activated 90 kDa ribosomal S6 kinase. EMBO J. 16:3133–3144.
44. Shimojima, M., T. Miyazawa, Y. Ikeda, E. L. McMonagle, H. Haining, H. Akashi, Y. Takeuchi, M. J. Hosie, and B. J. Willett. 2004. Use of CD134 as a primary receptor by the feline immunodeficiency virus. Science 303:1192–1195.
45. Shimojima, M., T. Miyazawa, Y. Sakurai, Y. Nishimura, Y. Tohya, Y. Matsuura, and H. Akashi. 2003. Usage of myeloma and panning in retrovirus-mediated expression cloning. Anal. Biochem. 315:138–140.
46. Shinya, K., S. Hamm, M. Hatta, H. Ito, T. Ito, and Y. Kawaoka. 2004. PB2 amino acid at position 627 affects replicative efficiency, but not cell tropism, of Hong Kong H5N1 influenza A viruses in mice. Virology 320:258–266.
47. Subbarao, E. K., W. London, and B. R. Murphy. 1993. A single amino acid in the PB2 gene of influenza A virus is a determinant of host range. J. Virol. 67:1761–1764.
48. Talon, J., C. M. Horvath, R. Polley, C. F. Basler, T. Muster, P. Palese, and A. García-Sastre. 2000. Activation of interferon regulatory factor 3 is inhibited by the influenza A virus NS1 protein. J. Virol. 74:7989–7996.
49. Wang, X., M. Li, H. Zheng, T. Muster, P. Palese, A. A. Beg, and A. García-Sastre. 2000. Influenza A virus NS1 protein prevents activation of NF-κB and induction of alpha/beta interferon. J. Virol. 74:11566–11573.
50. Wei, L., M. R. Sandbulte, P. G. Thomas, R. J. Webby, R. Homayouni, and L. M. Pfeffer. 2006. NFkappaB negatively regulates interferon-induced gene expression and anti-influenza activity. J. Biol. Chem. 281:11678–11684.
51. Wright, P. F. 2007. Orthomyxoviruses, p. 1691–1740. In D. M. Knipe, P. M. Howley, D. E. Griffin, R. A. Lamb, M. A. Martin, B. Roizman, and S. E. Straus (ed.), Fields virology, 5th ed. Lippincott Williams & Wilkins, Philadelphia, PA.
52. Wurzer, W. J., C. Ehrhardt, S. Pleschka, F. Berberich-Siebelt, T. Wolff, H. Walczak, O. Planz, and S. Ludwig. 2004. NF-kappaB-dependent induction of tumor necrosis factor-related apoptosis-inducing ligand (TRAIL) and Fas/FasL is crucial for efficient influenza virus propagation. J. Biol. Chem. 279:30931–30937.
53. Zykova, T. A., F. Zhu, Y. Zhang, A. M. Bode, and Z. Dong. 2007. Involvement of ERKs, RSK2 and PKR in UVA-induced signal transduction toward phosphorylation of eIF2alpha (Ser(51)). Carcinogenesis 28:1543–1551.